WAKE OF SLOT JET STUDIES

by

Shyamal K. Ghosh

A thesis submitted to the

Department of Chemical Engineering

of the

University of Ottawa

in partial fulfillment of the requirements

for the degree of M.Sc.

Thesis Author

Research Director

TABLE OF CONTENTS

ACKNOWLEDGEMENT

The author wishes to express his indebtedness to Dr. Benjamin C.-Y. Lu, Head of the Department of Chemical Engineering, for his guidance and encouragement in carrying out the research project for this thesis.

Many thanks are also due to Mr. G. A. Campbell, graduate student of the Department, for his useful suggestions and assistance in experimental work, and also to Messrs. F. Giacobbi and G. Gasperetti, technicians of the Department, for constructing the experimental apparatus.

ABSTRACT

Flow patterns developed by the inclined slot air jets, injected in a main air stream flowing at different velocities from 132.5 - 208 feet per second in a four-inch square duct, were studied from numerous pressure probe readings. Velocity profiles across the width of the duct at various positions were obtained from the readings on a recorder chart, given by the travelling probe.

An elliptical shaped zone of air recirculation was indicated from the velocity readings at different points.

Several correlations were obtained to predict the area and the position of the zone of recirculation, when the fluid properties in the jet stream and the main stream are known.

From the data obtained in this experiment, the similarity drawn between the jet fluid obstruction and the bluff-body obstruction, seemed to be somewhat questionable.

INTRODUCTION

One of the major problems of combustion in a high velocity gas stream is to maintain a stable flame. The flame tends to blow off after a certain velocity of the main stream is attained. Thus in recent years much studies have been made on the phenomenon of flame stabilization.

The established method of obtaining flame stabilization is known as bluff body flame stabilization. In this technique a bluff body of suitable geometrical shape is placed in the main stream, and thereby it creates a physical obstruction to the main flow. The existence of the bluff body thus gives a zone of recirculation behind its wake. The flow in this zone of recirculation is very much different than that in the main stream. Hence a stable flame can be maintained in this zone of recirculation; and this flame then helps to ignite the surrounding stream. However, this bluff body method of flame stabilization has the following disadvantages, which should be reduced or eliminated.

a) Much pressure energy is lost by the drag of the bluff body.

b) The dimensions of the bluff body depend on the main stream velocity.

c) The existence of a bluff body in the centre of a combustion duct brings in much mechanical complications.

Hence the ideal properties of a flameholder should be as follows:

a) The flameholder should be removable, when the main stream flow is low enough to have no requirement of flame stabilization.

b) The flameholder should have variable properties with regard to pressure loss, so that by adjusting the flameholder the pressure loss would be the minimum required.

The requirements of the above two properties bring in the idea of gas jets, which can be both variable and removable, as flame stabilizers.

Purpose and Scope of Investigation

Gas jets can be put through slots at the centre of the main stream flow. However, this arrangement again brings some mechanical complication of the operating system. Whereas, if the jet is injected from the centre of the wall of the flow system, no such complication is encountered.

One important thing that one should bear in mind at the very beginning is that for flame stabilization the creation of a recirculation zone in the wake of a flameholder is only a necessary, but by no means sufficient, condition. The engineering aspects of flame stabilization fall into two main categories.

a) The fluid dynamics aspect

b) The chemical-kinetics aspect.

The existence of a recirculation zone only satisfies the fluid-dynamics aspect of flame stabilization. Thus a recirculation zone does not necessarily guarantee a stabilized flame. On the other hand, without a recirculation zone flame stabilization is not possible.

In this investigation, mainly the flow characteristic in the

wake of a rectangular slot jet was studied. The angle of injection of the jet was at 45°, directed against the direction of the unidimensional main stream flow. Air was the experimental fluid in both the main and jet streams.

LITERATURE SURVEY

Earlier studies concerned with the injection of fluid jet in a main stream were done mainly to observe the diffusion of the jet fluid in the main stream. Here the main concern was to obtain the outer boundary of jet flow path, by various experimental techniques.

Chilton and Generaux (1) studied photographically the mixing effect of two dimensional slot jets in a 1.75" diameter glass tube using carbon dioxide, sulfur dioxide, nitrogen or air, both as the jet fluid and the main fluid. Titanium tetrachloride was added to the jet gas to produce a visible smoke. They concluded that the ratio of the mass velocity of the main stream gas to the mass velocity of the jet stream gas is the most important factor governing the quality of mixing, and suggested that with an ordinary T-connection good mixing can be obtained by making the mass velocity of the added stream two to three times that in the main stream.

Hawthorne, Rozers and Zackzek (2) studied the penetration and mixing of a jet of cold air issuing through a hole in the wall of a 3" square duct carrying hot air. Temperature rake measurements, shadowgraph and schlirien photographs were taken. The penetration increased if another rod or jet was placed immediately upstream. A jet from a square hole gave the same penetration as the jet from a circular hole of same area. The jet from the rectangular hole penetrated more in the main stream when placed with its long side in the direction of the main stream flow, and penetrated less when placed transversely.

Chelko (3) studied the penetration of water jets into a high velocity air stream. Penetration readings were taken photographically through the transparent tunnel walls made of lucite. The air velocity was maintained constant at 742 feet per second while the jet velocities varied from 168.1 to 229 feet per second. The range of the jet diameters was from .0135 inch to .0625 inch. By means of dimensional analysis, he obtained the following correlation from his experimental readings.

$$\ell / D_j = .450 \, (V_j/V_0)^{.95} \, (\rho_j/\rho_0)^{.74} \, \left(\frac{S}{D_j}\right)^{.22} \qquad (1)$$

where ℓ = the penetration length

S = the mixing distance, which is the horizontal distance from the point of injection to the point where the penetration length is being measured.

V, ρ, D, - refer to velocity, density and diameter, respectively.

Subscripts 0 and j - refer to the main fluid and jet fluid, respectively.

Callaghan and Ruggeri (4) studied the penetration of circular air jets injected perpendicularly to the main air stream. Hot air jets were used and the penetration was measured by means of thermocouple rake. They defined the penetration point as the point where the temperature is 1°F above the free stream total temperature. Velocity of the air stream used was from 260 to 360 feet per second, and the air jet temperature was 400°F. Four different jets of diameters .25", .375", .500", .625"

were used. The final correlation given by them using the same nomenclature as Chelko (3), is

$$\left(\frac{\ell}{D_j}\right)^{1.65} = 2.91 \frac{\rho_j V_j}{\rho_0 V_0} \sqrt{\frac{S}{D_j}} \qquad (2)$$

Callaghan and Bowden (5) studied the penetration of air jets issuing from circular, square and elliptical orifices directed perpendicularly to the main stream. They concluded that

a) Greater penetrations were obtained with square orifices than with circular orifices of equal area.

b) At low tunnel velocities and low jet pressures, greater penetrations were obtained with the square orifices and the elliptical orifices having an axis ratio of 4:1 than with other orifices investigated.

c) The square orifices gave the best penetrations at the higher values of tunnel air velocities and jet total pressures.

The experimental conditions in this study were

a) Tunnel air velocities - 160, 275 and 380 feet per second.

b) Circular orifice diameters - .375", .500", .625".

c) Ellipse axis ratios - 2:1 and 4:1.

d) Areas of squares and ellipses - Area of .375" diameter and .625" diameter circles.

Miller, Foster, Ross and Wohl (6) observed the mixing of air stream with a jet of carbon dioxide in square ducts of 1", 2", and 3" square areas. In some experiments also the roles of the gases were

inverted, i.e. carbon dioxide was used as the main stream and air as the jet stream. Experimental data were taken by means of shadow photographs and also by chemical analysis. Circular, square and rectangular injectors were used. The correlation obtained was

$$P/D = K_p/R_m^2 \, R_v \qquad (3)$$

where R_m = mass velocity ratio of the side stream to the main stream

R_v = volume flow ratio of the side stream to the main stream

P = the longitudinal distance between the jet and the place where the jet just reaches the top wall or roof (this parameter is a measure of the stiffness of the jet or its resistance to being bent)

D = diameter of the main duct in inches

K_p = constant

Gordier (7) used a 12" x 18" gravity water tunnel (water flow maintained by the force of gravity). The jet liquid was tap water and the tunnel liquid was river water. Dye was injected to the jet liquid and both water and water-air mixture were used as jets. Data were taken photographically with the help of the coloured water jets. Photographs of both the vertical penetration and the lateral spread of the jet were taken. From his experimental data, Gordier concluded that

a) the tests conducted in a water tunnel verified the N.A.C.A. (4) penetration data at jet to channel velocity ratios less than six. At higher values of the said ratio a secondary effect other than jet

Reynolds number is present to cause deeper penetration than previously predicted (4).

b) the maximum lateral spread of liquid jets discharging into the same liquid is given by

$$Z/D = 0.6\ V_j/V_0\ (S/D)^{.39} \qquad (4)$$

where Z = one half the maximum jet width at a distance downstream

V_0 = main tunnel liquid velocity

D = jet diameter

V_j = jet liquid velocity

Chakko (6) injected hot subsonic jets into cold air streams and measured the penetration by means of thermocouple. From his data he gave the following correlation:

$$H_c/D_j = .945\ (V_j/V_0)^{.612}\ (T_0/T_j)^{.172}\ (S/D_j)^{.265} \qquad (5)$$

where H_c = penetration length of the hot jet

D_j = jet diameter

V_j = jet velocity

V_0 = mainstream velocity

T_0 = mainstream fluid temperature

T_j = jet fluid temperature

S = the mixing distance

Beauregard (9) also used temperature rake to measure the penetration of cold air jet in hot high velocity main air stream. From his data he produced many curves showing the actual penetration.

Ehrich (10) used the potential flow theory for his analysis of the dynamics of slot and orifice jets injected at different angles to the main stream flow. His analysis showed qualitative agreement with Callaghan and Ruggeri's (4) data for jet penetration.

Frazer (11) also analysed the penetration of circular jets at right angles to the main stream flow, and agreed with Callaghan and Ruggeri's (4) data.

When high speed combustion took its important place in technology due to the rapid advance of jet engines, much research work was started on the flame stabilization in high speed flow. It was known long ago (12) from the study of fluid dynamics that recirculation of fluid flow takes place in the wake of a bluff body when it is placed in a high velocity fluid stream.

In order to understand the action of bluff body flameholders, one should consider some facts concerning the flow of fluid around a solid obstacle, e.g. a cylinder in a stream. At the upstream face of the cylinder the fluid is dammed up so that the stream tubes enlarge in cross section; the velocity decreases and the pressure increases according to Bernoulli's principle. The stagnation point where the fluid comes entirely to rest and the pressure attains a maximum is at the cylinder surface in the centre of the dammed up region. The flow around

the cylinder is accelerated by the pressure developed; and as the fluid accelerates the pressure decreases. When the flow around the cylinder becomes parallel to the main stream flow, maximum velocity and minimum pressure are obtained. The flow would close up behind the cylinder in the same way as it opened up in the front, in the case of ideal frictionless fluid in potential flow. For real fluids such symmetry is not obtained because a retarded boundary layer is formed at the surface of the body. This retarded boundary layer does not change the flow character on the upstream side, as the pressure gradient acts in the direction of motion. Whereas on the downstream side the retardation of the fluid affects the slower moving particles in the boundary layer more strongly than the particles in external flow. While the latter are enabled by their greater supply of kinetic energy to flow on, the former cannot overcome the opposing pressure gradient and finally, when all their kinetic energy has been consumed, they are made to turn back. Thus there occurs a flow in the reverse direction close to the boundary. More and more retarded fluid is piled up in a short time between the boundary and the external flow, so that the backward flow rapidly broadens out and the external flow becomes detached from the boundary. The layer of discontinuity then rapidly coils itself up into an eddy. The retarded material which is thus set in rotation as a result of friction is partly retained in the core of the eddy.

If the Reynolds number is sufficiently low, the eddies do not grow indefinitely, but form two symmetrical standing vortices at the

downstream face which rotates in roller bearing fashion (13). With further increase in Reynolds number, an increase in stagnation pressure takes place which causes the vortices to increase in size. The vortices elongate, eventually become distorted and break down. Ultimately vortices are shed alternately and at regular intervals from the sides of the cylinder, forming the well known Karman vortex street described in fluid dynamics text books.

At a still higher Reynolds number of about 10^5, another important change in the flow pattern occurs - the boundary layer becomes turbulent and the point of detachment shifts further upstream.

When a combustion wave attaches itself to an obstacle in the stream, a decrease of the downstream stagnation pressure occurs as a result of pressure drop across the wave. Thus, flame attachment acts in a way similar to reduction of Reynolds number. This mechanism readily explains the reduction of eddy size on flame attachment. Scurlock (14) used flames of city gas or propane with air produced in a transparent rectangular duct 3" by 1" cross section and about 18" long. The gas mixture was led into a calming chamber in which the flow cross section expanded from a 2" square section to a 15" square section over a length of 36" and residual turbulence was dampened by a series of fine wire screens. From the calming chamber the mixture was led through contraction to the observation section. The flame was stabilized V-shaped about 80 mesh diameters from the turbulence producing screens on various obstructions. Under Scurlock's (14) experimental conditions, it was

found that eddies were shed from the stabilizers before ignition, but no eddy shedding took place once the flame was formed.

Williams, Hottel and Scurlock (15) also studied the stabilization effects of variously shaped objects, such as rods and gutters, placed perpendicularly to the gas flow. They observed that there exists a region of high shear stresses between the mixture stream moving rapidly and the fluid decelerated in the boundary layer formed on the bluff body. These shear stresses cause the shedding of eddies downstream of the flame holder, and there occurs a reversed flow.

Some exploratory work on the flow in the wake of baffles was performed by Nicholson and Fields (16). They studied the intensity of mixing in the wake of baffles by taking high speed motion pictures. The characteristic light emitted by sodium vapour was used as tracer. In their experiment they found that for a 0.75" gutter placed in the main stream of 200 feet per second velocity, the average residence time of a particle in the recirculation zone was .008 second. The sodium vapour from the particles entering into the recirculation zone diffused completely throughout the zone in about .0002 second. Thus the ratio of the mixing time to the residence time was found to be about 1 in 40.

Longwell, Frost and Weiss (17) studied some detail of combustion in the wake of V-shaped baffle. They measured the combustion efficiency by taking time average measurements of oxygen consumption in stoichiometric fuel-air mixture. A combustion zone of high efficiency approximately the width of the baffle seemed to exist in the wake of the

baffle. This zone narrows down in the immediate downstream, but further downstream it expands again. By probing with a salt covered rod it was found that the combustion zone upstream of the rod was coloured yellow if the rod was not more than about 10.5" downstream of the baffle. This gave a recirculation zone length of 4-5 baffle diameters for the 2 1/4" gutter used. It was felt that this general pattern is typical of large size baffles placed in high velocity air streams.

Zukoshi and Marble (18) injected salt water solution from a very small tube and at low velocity into the wake of rod flame stabilizer. The resulting flow pattern was photographed and observed. They were mainly interested in the length of the recirculation zone, which they defined with great accuracy considering the complexity and irregularity of the wake flow. When the salt solution was injected downstream of the end of the recirculation zone, no luminar material appeared in the vicinity of the flameholder. If the point of injection was moved slightly forward, the entire recirculation zone appeared luminous. According to them, the length of the recirculation zone was found to vary as the square root of the characteristic flameholder dimension. They defined the ignition delay time or the characteristic time τ as

$$\tau = \frac{L}{V_{B_o}} \qquad (6)$$

where V_{B_o} = blowoff velocity determined experimentally

L = recirculation length

The blowoff condition is then defined by

$$\frac{V_{B_o}}{L} = 1 \qquad (7)$$

Zukoski and Marble (18) suggested that the flow immediately downstream of the flameholder is laminar at low Reynolds number, and in this case mass transport into the wake of the flameholder occurs by molecular diffusion. Whereas at high Reynolds number, when the flow is turbulent, mass transport by turbulent exchange occurs.

Westenberg, Berl and Rice (19) gave the results of helium tracer and combustion efficiency measurements made in the wake of a conical, 1-inch flameholder. The studies were carried out in very lean pentane-air flames stabilized at the exit of a 6-inch pipe in flows of 20 and 53 meters per second. The data obtained were interpreted as showing the lack of violent mixing existing in the recirculation zone, and the significance of the results were discussed qualitatively in the light of various theoretical models which had been proposed. Some additional experiments on stability and recirculation zone length were discussed briefly.

Williams and Maddocks (20) discussed the effect of stabilizer dimensions. They used rod flameholders of 1/50" diameter to 1/2 diameter, and concluded that

a) Increase in rod diameter results in a reduction of the rich stability limit and of the maximum attainable velocity.

b) Increase in rod diameter results in a curtailing of the lean limit of rod sizes up to 1/4" diameter and an extension of the lean limit for rods of larger diameter.

Wilkerson and Fenn (21) determined the effect of flameholder geometry on combustion efficiency in ducted burners. Stoichiometric mixtures of air and pentane at a flow rate of about .85 lbs. per second was passed through a two-inch round duct. The flameholder was a thirty degree cone whose diameter was varied from 0.5 to 1.125 inches. The ability of various flameholder configurations to mix with the pilot heat with the stream was determined by means of thermocouple traverses downstream of the igniter structure with the air flowing through the burner and only the pilot burning. A number K, with the dimensions of conductivity, and in effect the diffusivity of the stream, was thus associated with each configuration. A simple correlation between K and the combustion efficiency was then possible. K was defined as

$$K = \frac{q}{4\pi XT} \qquad (8)$$

where q = rate of heat input in BTU/sec.

X = distance in inches along burner axis downstream from igniter

T = temperature at distance X in degree Fahrenheit.

The final correlation was given by

$$\log \eta_c = \log A - \frac{E}{R} \frac{1}{(660 + ChK)} \qquad (9)$$

where h = pilot heat per cent = $\frac{\text{theoretical pilot heat}}{\text{theoretical fuel heat}} \times 100$

The evaluation of C was by trial and error. A value of 10^6 fitted the data very well.

The quantities A, E and R have the same meaning as in Arrhenius rate equation.

Dezubay (22) attempted to establish the groups of variables expected to control flame stability. He gave a correlation showing the effect of baffle diameter, pressure, and mixture velocity using propane as fuel. Fuel-air ratio at blowout was plotted as a function of the dimensional group $V/p^{.95}\ D^{.85}$ where

D = the diameter of the circular flat disks used to stabilize the flame

V = velocity past the baffle

P = pressure

T = absolute temperature.

Larger disks, higher pressures and lower velocities gave wide stability limits and a maximum value of the above group for stable operation was found in the region of stoichiometric amount of fuel-air ratio.

Haddock (23) also gave correlations of the effect of flame-holder diameter and blowout velocity. Cylinders with axis perpendicular to the flow and of diameters .494 to .89 inch were used as stabilizers. The velocity of the C_6-C_8 fuel ranged from 60 to 740 feet per second. He recommended the correlating group to be $V/D^{.5}$.

Longwell, Chenevey, Clark, and Frost (24) used cylinders (axis parallel to flow), cones, annuli V-gutters as flame stabilizers;

the C_5-C_8 fuel mixture velocity ranged from 200 to 950 feet per second. They recommended the correlating group to be V/D, D being the characteristic dimension.

William, Woo and Shipman (25) studied the boundary layer effects on stability characteristics of bluff-body flameholders. They concluded that this role of boundary layer is twofold. The aerodynamic character of the zone of contact between the burned gas and in the immediate wake of the stabilizer and the unburned feed stream gas is determined by the boundary layer; and also the presence of the boundary layer means that the unburned gases coming into the zone of initial combustion have been preheated. The relatively slow movement of the boundary layer only influences the character of the zone of contact between the burned and unburned gas. This dual role is further confirmed by the effect of the boundary layer removal on the stability limits.

The idea of a rotating flameholder was experimented by Grover, Kesler and Scurlock (26). The flameholder used was a metal cylinder placed longitudinally in the fuel stream. The combustion efficiency increased with increased rate of rotation; and the flame shape was helical. Power loss was less than that due to the axial drag. However, the main disadvantage experienced was that the stability limits were narrowed.

Recessed ducts in the wall of the combustion tunnel as a means of creating flame stabilization was tried by Huellmantel, Ziemer, and Cambel (27). This device provided an ignition nucleus. However, the

main disadvantage of this scheme was the creating of high temperatures at the wall.

Spalding (28) put forward the idea of creating a zone of recirculation as in the case of a bluff-body flameholder by purely aerodynamics means. He suggested the injection of a jet normal to the main gas stream flow. This method has the advantages of easy control of the recirculation zone independent of the main stream properties.

Shepherd (29) studied flame stabilization by means of annular fluid jets. He obtained flame stabilization data for propane-air mixtures in an annular duct, the stabilization being obtained by the injection of pure air or of a stoichiometric propane-air mixture perpendicularly outwards into the main stream from the inner tube of the annulus. The annular injection gap width varied from .010 to .030 in. The duct was 2.375 in. I.D. with the inner injection tube 1/2 in. in diameter. He concluded that flame stabilization is possible by means of annular fluid jets with relatively narrow injection widths and low rate of injection flow.

Dutta, Martin, and Moore (30) also made a study of flame stability in ducts by injecting jets perpendicularly inwards into the main stream. The main burner tube consisted of two lengths of stainless steel tubing 1.375 in. internal diameter. An adjustable annular gap was arranged by separating the burner tubes with the help of threaded sleeve. The gap could be supplied with either a metered stream of air or a combustible mixture. Their results agreed to those obtained in the

parallel investigation by Shepherd (29).

A correlation between jet velocity and the main stream velocity at blowout applied over a range of jet velocities and jet widths. Certain similarities had been shown to exist between the jet stabilized system and conventional bluff-body stabilizers by correlating the results in terms of Peclet numbers.

A discussion of high intensity combustion systems with recirculation by means of induced air has been given by Clarke (31).

Schaffer and Cambel (32, 33) found that the performance of an opposing jet flameholder is better than some types of physical flameholders, under certain circumstances. They also observed that the blowout curves could be shifted considerably by using fuel-air jets. They introduced the concept of the critical zone, defined by them as a small pilot reactor from which the flame spreads; and they suggested that the conditions in this zone determine whether or not the flame will be stabilized.

The effect of jet size and jet pressure on the flame stabilization of an opposing jet using a propane-air mixture as the jet fluid was studied by Pohlmann (34).

Golitzine (35) found that kerosene, injected upstream by an air jet, would produce flame stability without the use of baffles in the main air stream. The flame stability limits were found to be narrowed by an increase in main stream velocity, as well as by a decrease in main stream static pressure; the stability limits were found to be widened by an increase in air blast pressure and flow.

From their study of flame stabilizing effects of inclined air jets, Duclos, Schaffer and Cambel (36) arrived at the following conclusions.

a) The flame holding ability of the single opposing jet tested decreased rapidly with the increase of the incidence angle from 0°.

b) Multiple non-coverging jets did not give better results than a single jet at the same angle, although when the jets converge at a given angle, the flame holding ability improved greatly.

Bertin and Salmon (37) investigated the applications of transverse air jets as flame stabilizers. Satisfactory results were obtained, both at sea level and at altitude, when the process was applied to a turbo-jet engine afterburner; a fluid baffle rather than a simple fluid jet was used as the stabilizer. The total and the static pressures in the flow stream in the experimental duct were given by a complete set of pressure probes mounted on a movable board.

EXPERIMENTAL DETAILS

The equipment used in the whole experimental setup may be grouped under the following headings:

(1) Main Air Flow Equipment

(2) Jet Air Flow Equipment

(3) Device For Taking Experimental Readings.

(1) Main Air Flow Equipments

A - The Blower - The capacity of the Buffalo High Pressure Blower of model number 28HU-DBS used for supplying the main stream was one thousand cubic feet per minute at forty-five inches of water. This was capable of producing a maximum velocity of about 250 feet per second through the experimental duct. The amount of air supplied by the blower was controlled by an inlet damper.

B - Sound Proofing - As the blower for the main air supply produced much noise, it was decided to keep the sound to a minimum. The blower was mounted on concrete foundations and four vibration damping mounts were placed at four corners of the blower base. A cubic box of 6' side made of low density fibre-board enclosed the blower; a vertical four inches wide opening on one side allowed air to be drawn by the blower. The outlet of the blower was connected to the main duct section with a flexible rubber coupling.

C - Section For Smoothing The Flow - To make the air flow from the blower smooth, a galvanised pipe of four inches diameter was added to the flexible rubber connection from the outlet of the blower.

A minimum upstream distance of twenty diameters from the measuring station is required for the flow to be smooth.

D - Main Duct - This main duct where the actual experiment was performed, was a four inch square duct with 1/4 inch thick steel walls. Numerous holes were drilled on one wall in the main experimental section of the duct. Instead of threading the holes, they were reamed with a ten degree tapered reamer, and tapered pins were used to close the holes. This device of making holes increased the number of measuring points per unit area of the wall. Each time only one pin was withdrawn to insert the probe, thus the main duct was virtually closed against air leak.

E - Exhaust Air - The air from the experimental duct was exhausted through an old chimney, the base of which was connected to the rear end of the experimental duct.

(2) Jet Air Flow Equipments

A - Compressors - For supplying the compressed jet air flow one Gardiner Denver of model number 254U-DBS and another Ingersoll Rand of model number 71-TD compressors with a supply pressure of 125 psig were used. The total capacity obtained from the two compressors was fifty-seven standard cubic feet per minute.

B - The Pressure Regulator - To maintain the pressure constant during experimental measurement, a constant pressure valve of model number 42H100 from the Moore Regulating Company was fixed in the air line supplying the jet air.

C - The Jet Injector - The injector was a rectangular slot of given dimensions drilled at an angle of incidence of 45° in a flat, round 1/4 inch thick piece of steel plate. This steel plate of 1" diameter was threaded on the edge, and was screwed into the hole in the top wall of the duct. A gasket was used to make the steel plate base flush with the duct wall. On this round plate a 3" long, 3/8 inch diameter steel pipe was welded, and the pipe was connected to the air supply by a flexible metal hose. To make sure that the jet pointed in the right direction, a mark on the circumference of the round steel plate was made before screwing it into the hole. This technique of using jet air supply avoided drilling and plugging more than one hole in the main duct; the steel disc was replaced with another one when the injector was changed.

D - Flow Meters - Sharp-edged orifices and U-tube manometers were used to measure the air flow. The construction of the orifices and pressure tap connections was made according to the instructions given in Perry's Chemical Engineers' Handbook.

(3) Devices for Taking Experimental Readings

A - The Pressure Probe - For measuring the flow pressures in the entire cross section of the experimental station, a probe was made of a fifteen B.D. hypodermic needle with a small hole on the upstream side of the tip of the needle. The needle probe was soldered to a brass tube. The connections to the pressure recorders and the probe were made through copper and rubber tubings.

B - The Probe Carriage - A movable carriage was fixed to the probe, so that the probe can be placed in any point of the experimental station through any of the drilled holes on the side wall of the duct. The probe was made free of vibration resulting from the blower by means of an interlocking device. To permit a suitable movement of the probe along the width of the duct, a 1 r.p.m. synchronus motor was used. This motor was connected through rack and pinion gearing to the probe. By using suitable gear ratios, the movement of the probe was fixed to a constant speed of one inch in five minutes.

C - The Pressure Recorders - The pressure line from the probe was connected to two identical Brown pressure recorders of model number Y702X23-C38-11-111-(64)-SK999 by means of a T-connection. One recorder gave the positive readings from 0-10 psig, and the other gave the corresponding negative readings from 0-10 psig. Thus the use of two pressure recorders instead of one greatly facilitated the range of pressure readings.

Experimental Procedure

By adjusting the damper of the blower inlet, the velocity of the air flow in the main duct was regulated. The range of velocity used was from 132.5 to 208 feet per second. The jet air was supplied from the compressors at a desired pressure by operating the regulating valve. The jet air flow was measured from the U-tube manometer connected to the orifice taps. The velocity at any point in the duct was measured by means of the probe connected to the Pressure Recorders. The chart used

in the Recorders was a twenty-four hour chart. However, the twenty-four hour motors in the Recorders were replaced by two hour motors. This made the one hour divisions in the chart equivalent to five minutes. The probe was inserted fully through one of the holes. After allowing a couple of minutes for the pressure equilibrium to be reached, both the probe and recorder motors were started. The length of the probe needle was about three inches. Hence, it took about fifteen minutes for the probe to take velocity traverse across three inches of the duct width through one particular hole. This velocity traverse reading was spread out to three divisions on the chart; and from this chart, velocity at any point could be read. The procedure was repeated by using other holes, until a complete picture of the flow pattern in the wake of the jet was obtained.

Two different jet dimensions were used; one was 1/4" by 1/16" and the other was 1/4" by 1/8". The velocity of the main stream was varied from 132.5 feet per second to 203 feet per second. The jet pressure was varied from 5 pounds per square inch to 30 pounds per square inch. Both the jets were placed with their long sides against the direction of the mainstream flow.

To study the effect of the orientation of the jet with respect to the mainstream flow direction, a few sets of readings were taken with the 1/4" by 1/16" jet with its short side against the direction of mainstream flow.

Photograph and Diagram of the Experimental Equipment

The photograph and diagram of the experimental equipment are presented respectively in Figures 1 and 2.

Experiment for the Visualisation of Flow in the Wake of a Fluid Jet

At the beginning of the experiment, it was realised that the interpretation of the flow pattern in the jet wake from the pitot tube probe reading will suffer from one main disadvantage if there is no approximate idea of the main direction of flow in the jet wake. The pitot tube had one opening facing the mainstream flow. A streamline coming from a flow moving either from side to side (horizontally) or from top to bottom (vertically) with respect to the duct, which hits at the back of the pitot-tube opening, could not be distinguished from the pressure readings. Hence it was necessary to know whether the flow in the wake travels from side to side or from top to bottom.

For this purpose a supplementary experiment was performed with water jets injected from the top wall to the mainstream water flowing in a 2" square transparent lucite duct. Air which was sucked from the atmosphere by the water jet through a small opening before the injection point formed bubbles in the wake of the jet in the duct. The bubbles were observed to follow a semicircular path in the plane A-B-C-D (Figure 3). From this visual observation it was assumed that the flow path of the fluid particles in the wake lies on this plane and not on the plane a-b-c-d of Figure 3 as in the case of wake of a bluff body.

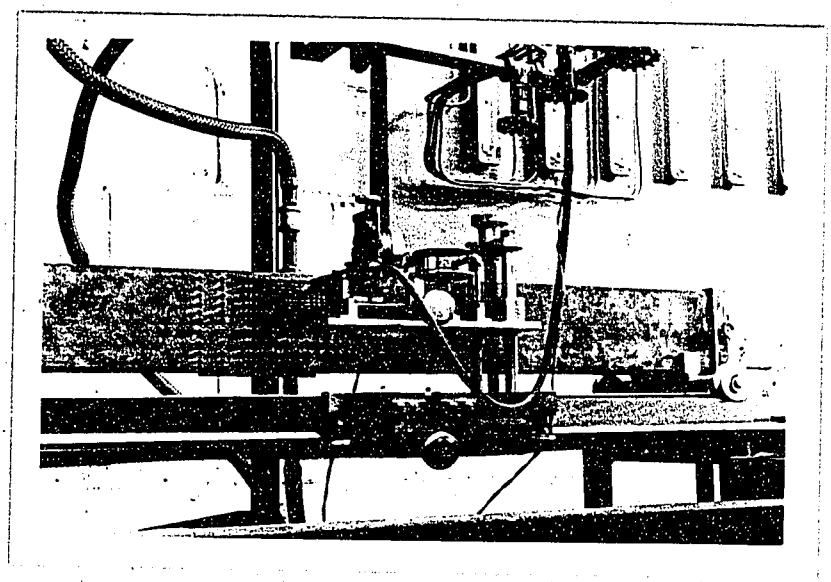

Fig. 1. A photograph of the four-inch square duct showing the working section, the pressure measuring probe and air injectors.

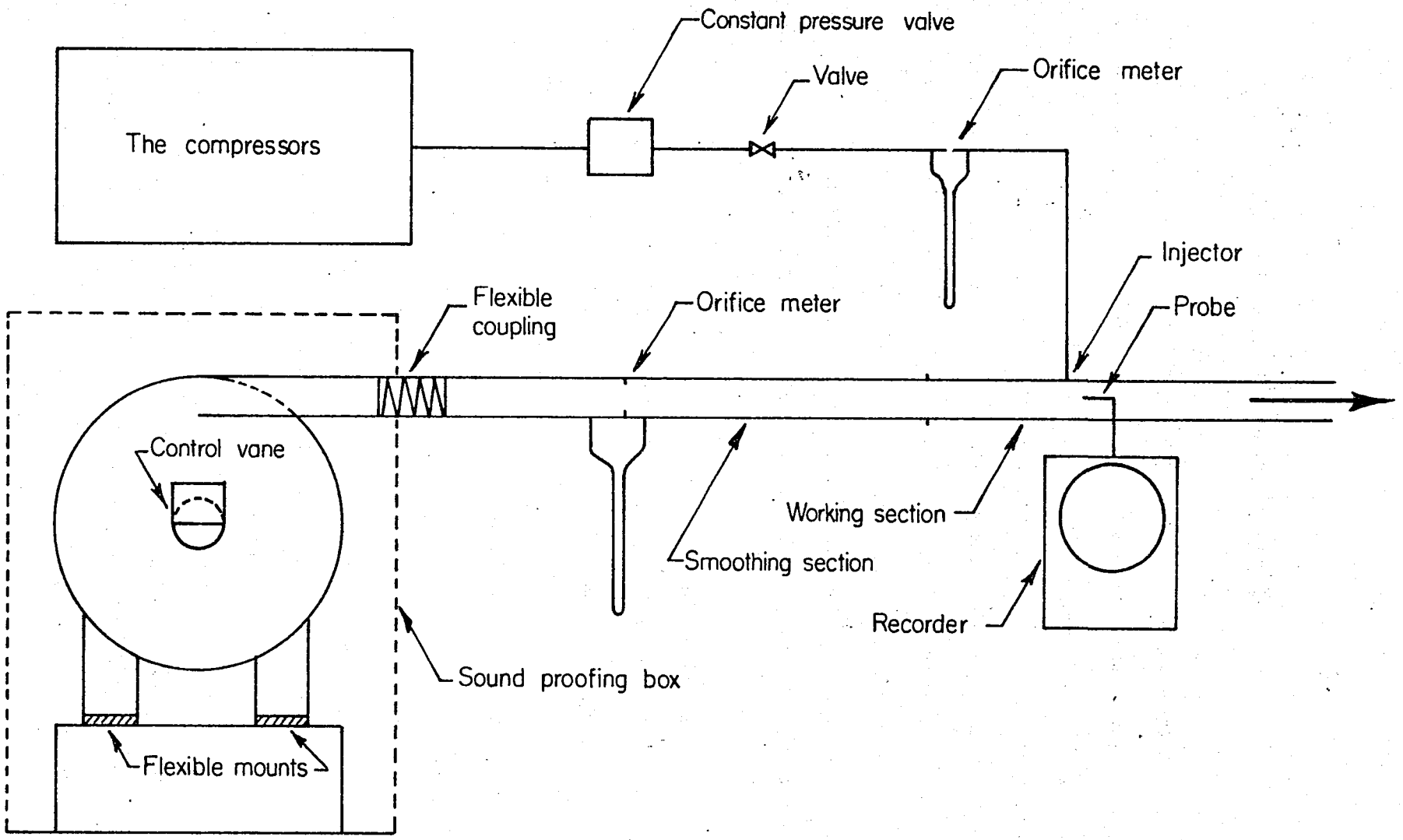

Fig. 2. Schematic diagram of the equipment

PRESENTATION AND DISCUSSION OF RESULTS

Velocities for different points at the central vertical plane A-B-C-D (Figure 3) were plotted. One such plot is shown in Figure 4. It is seen from this figure that within a certain enclosed space in the central vertical plane of the duct the point velocities everywhere are negative. However, outside this enclosed space (in the particular plane) the point velocities anywhere are positive. This observation indicates the presence of a recirculation zone in the wake of the fluid jet. The same type of observations is obtained with every other combinations of jet dimensions, jet pressures, and main velocities used in this experiment.

The presence of such a recirculation zone leads many workers (37) to compare the fluid jet obstruction with a bluff-body obstruction in the main stream. However, this comparison seems to be somewhat questionable for the following reasons:

1. In a horizontal line in the plane (Figure 4) the point velocity along the upstream direction of the main flow stream from the null velocity loop, at first increases slowly, and then increases rapidly until attaining the maximum negative velocity. This suggests the idea that at points immediately behind the jet, the fluid particles are experiencing some kind of sucking action.
2. That the flow in the present case is different from the case of a bluff-body is further justified by observing the motion of air bubbles, when a water-air mixture jet is injected in the main water

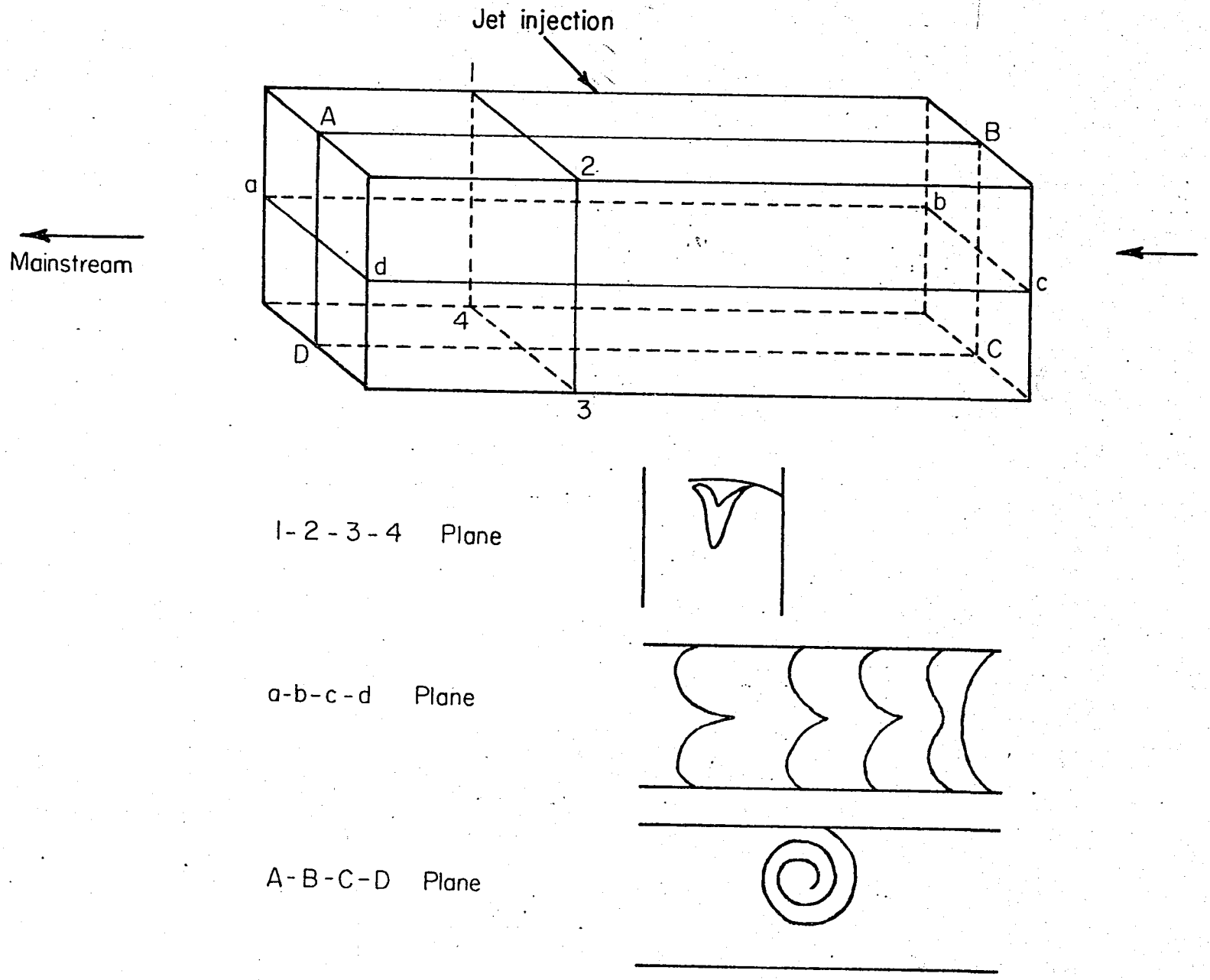

Fig. 3. Flow patterns in various planes

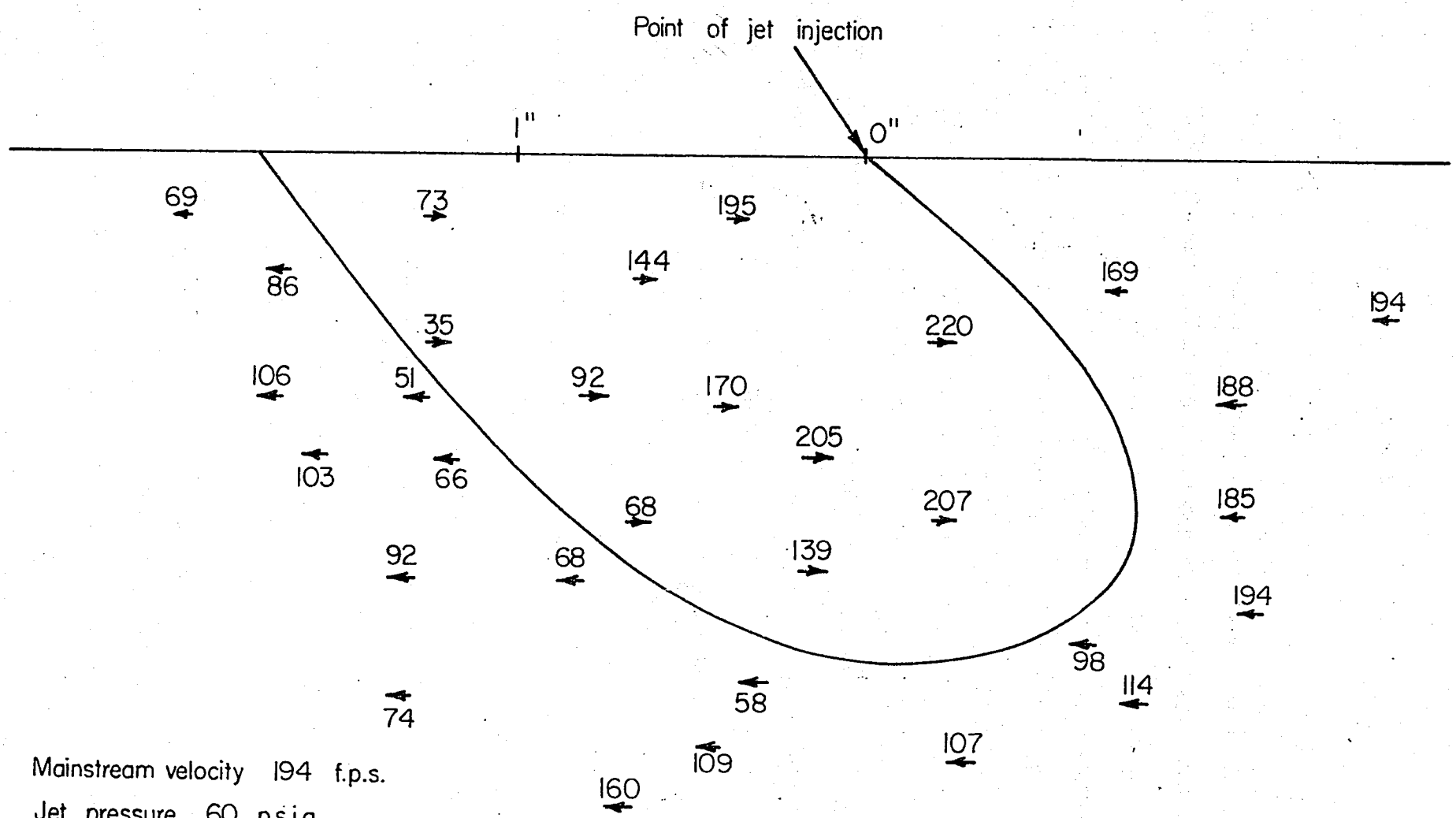

Fig. 4. Point velocities in the plane A-B-C-D at the centre of the duct width

stream. Observation of this kind was made to give an insight of the flow mechanism in the original experiment. The air bubbles in the wake of the jet were observed to follow both vertical and horizontal motion, going in an inclined fashion in the upstream direction of the main stream. This observation suggests that the jet fluid is being bent by the main stream flow after a certain vertical distance from the point of injection, and finally the jet fluid assumes a spiral form, as pointed out by Campbell (38).

The stagnation zone of the wake fluid is assumed to be an elliptical zone on the downstream of the wake, within which the point velocities given by the probe are less than approximately sixty feet per second. The centre of the stagnant zone then becomes the centre area of this elliptical zone. With this assumption about the stagnant zone, an attempt was made to describe this elliptical zone completely by describing its area A_Z, the horizontal inclination of the major axis of the ellipse α, the vertical distance of the lowest point of the major axis from the top wall y, and the horizontal distance from the point of injection to the point where the vertical line from the lowest point of the major axis touches the top wall x (Figure 5) when the velocities and densities of the main stream and the jet stream are known. The values of all the above quantities are given in Table I.

Correlation for the Area of the Elliptical Zone

By means of simple dimensional analysis involving all the variables that may be expected to affect the area of the stagnant zone,

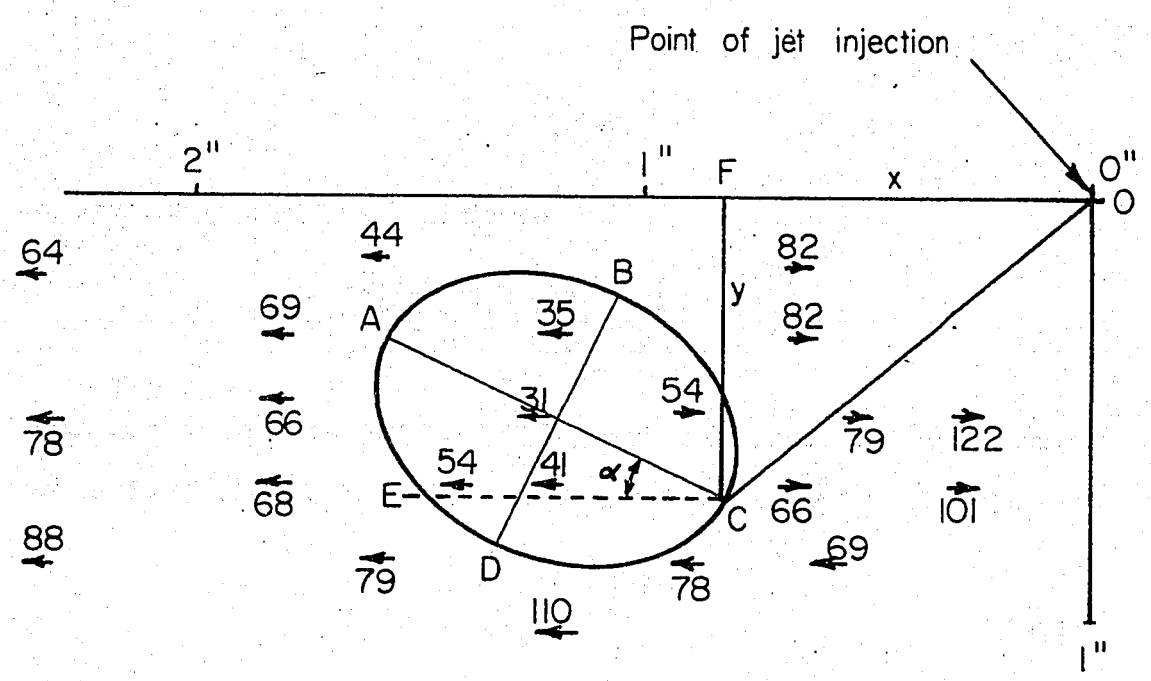

ABCDE — Stagnant eliptical zone

OF — x

FC — y

∠ACE — α

Fig. 5. Figure to show the different terms used in the correlations for describing the stagnant zone of recirculation

the following result was obtained:

$$\frac{A_z}{A_j} = K \left(\frac{\rho_j V_j \ell_j}{\mu_j}\right)^a \left(\frac{V_j}{V_0}\right)^b \left(\frac{\rho_j}{\rho_0}\right)^c \left(\frac{\mu_j}{\mu_0}\right)^d \qquad (10)$$

Neglecting the effects of the jet Reynolds number and the viscosity ratios the following equation for the present analysis was expected.

$$\frac{A_z}{A_j} = K \left(\frac{V_j}{V_0}\right)^b \left(\frac{\rho_j}{\rho_0}\right)^c \qquad (11)$$

where A_z = area of the stagnant elliptical zone, in square inches

A_j = area of the jet injector, in square inches

b, c, K = constants

V_j = velocity of the jet air, in feet per second

V_0 = velocity of the mainstream air, in feet per second

ρ_j = density of the jet air, in pounds per cubic foot

ρ_0 = density of the mainstream air, in pounds per cubic foot

The exact form of the equation is given as

$$\frac{A_z}{A_j} = 1.68 \left(\frac{V_j}{V_0}\right)^{1.75} \left(\frac{\rho_j}{\rho_0}\right)^{1.67} \qquad (12)$$

from the Figures 6 to 8.

That the effect of Reynolds number is negligible is further justified by the graphs in Figure 6. The points in each of the graphs represent two different Reynolds number, and yet a straight line could be passed through all the points. That is to say, no consistent trend

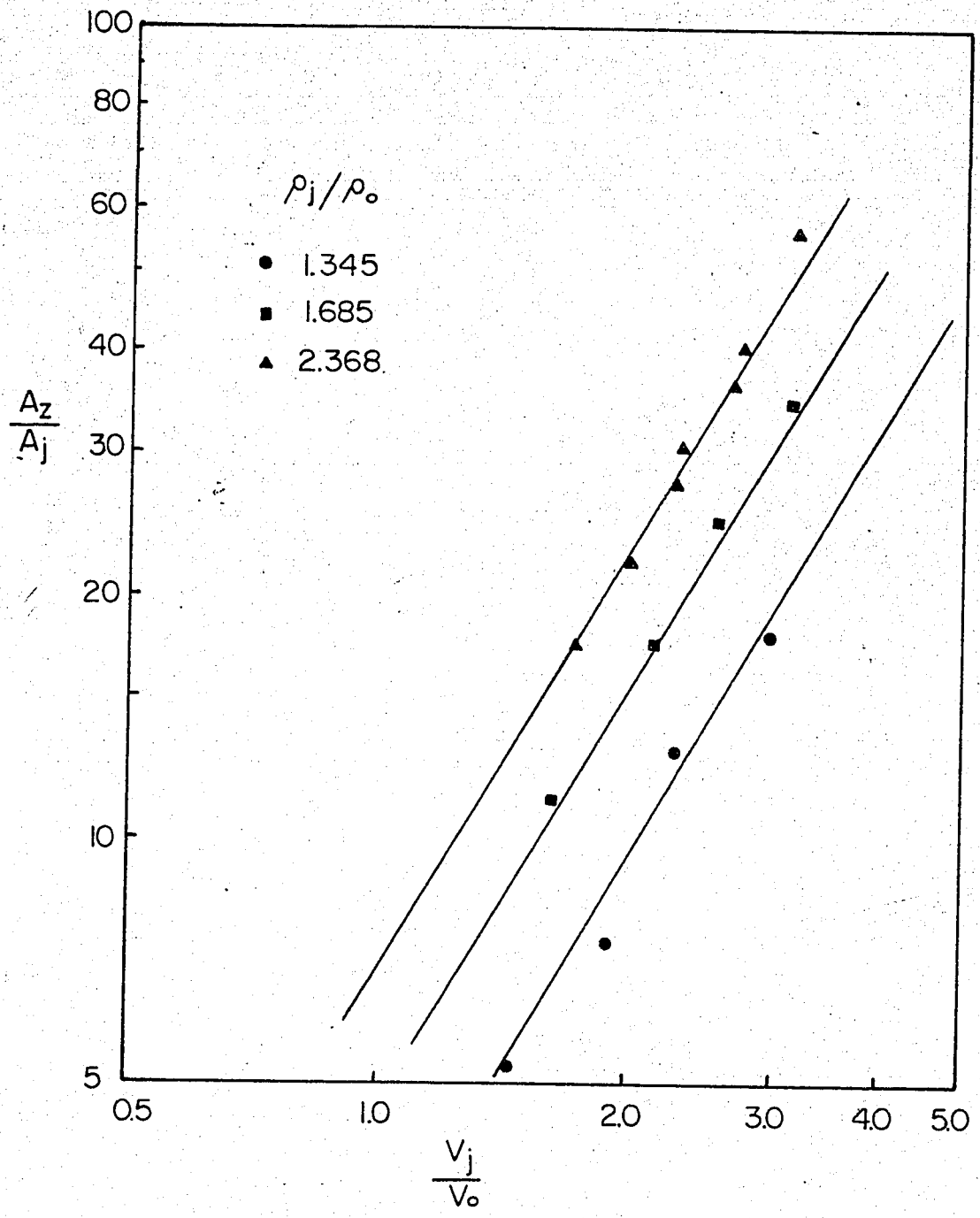
100
80
60
40
30
20
10
5
$\frac{A_z}{A_j}$
ρ_j/ρ_o
1.345
1.685
2.368
0.5
1.0
2.0
3.0
4.0
5.0
$\frac{V_j}{V_o}$

Fig. 6

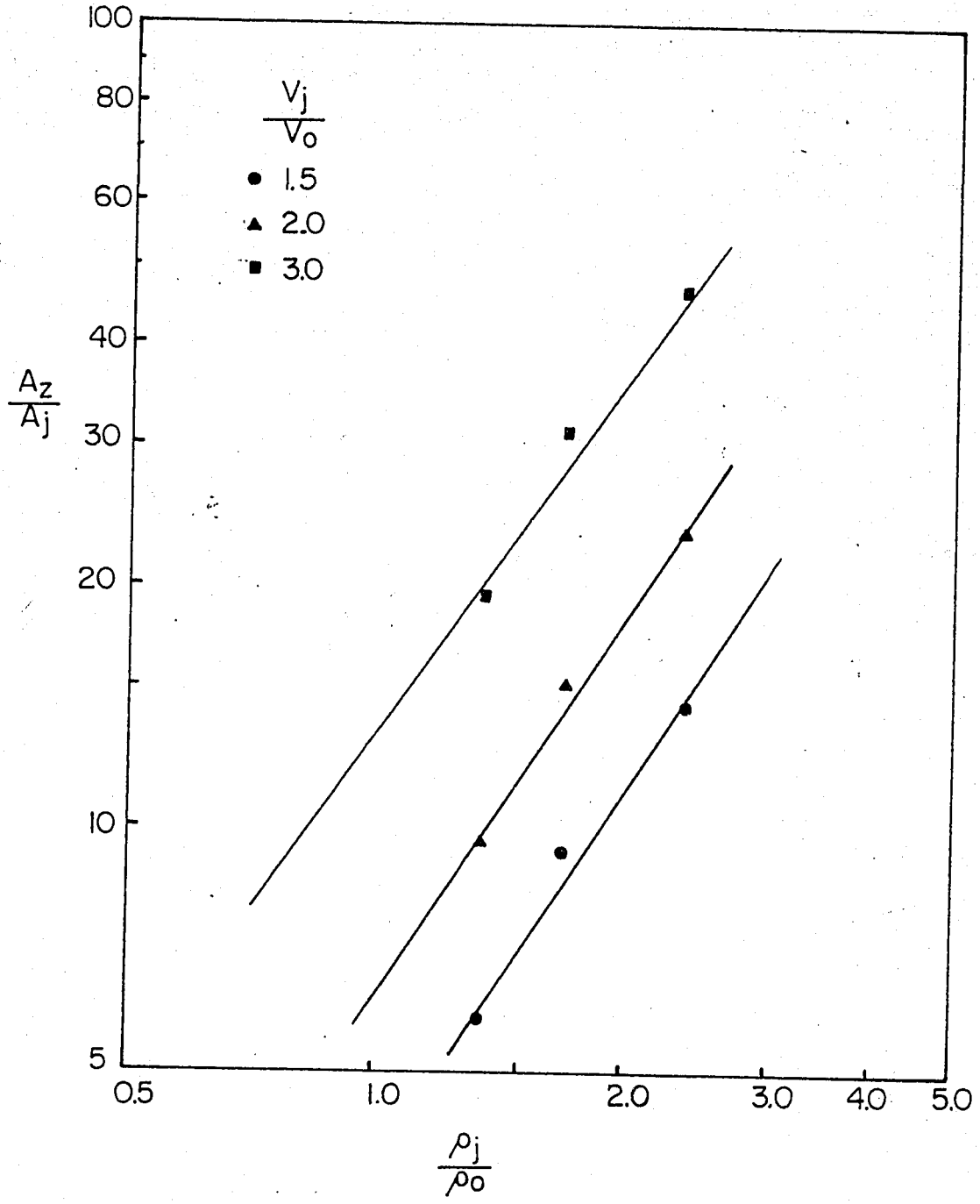
100
80
60
40
30
20
10
5
$\frac{A_z}{A_j}$
$\frac{V_j}{V_o}$
1.5
2.0
3.0
0.5
1.0
2.0
3.0
4.0
5.0
$\frac{\rho_j}{\rho_o}$

Fig. 7

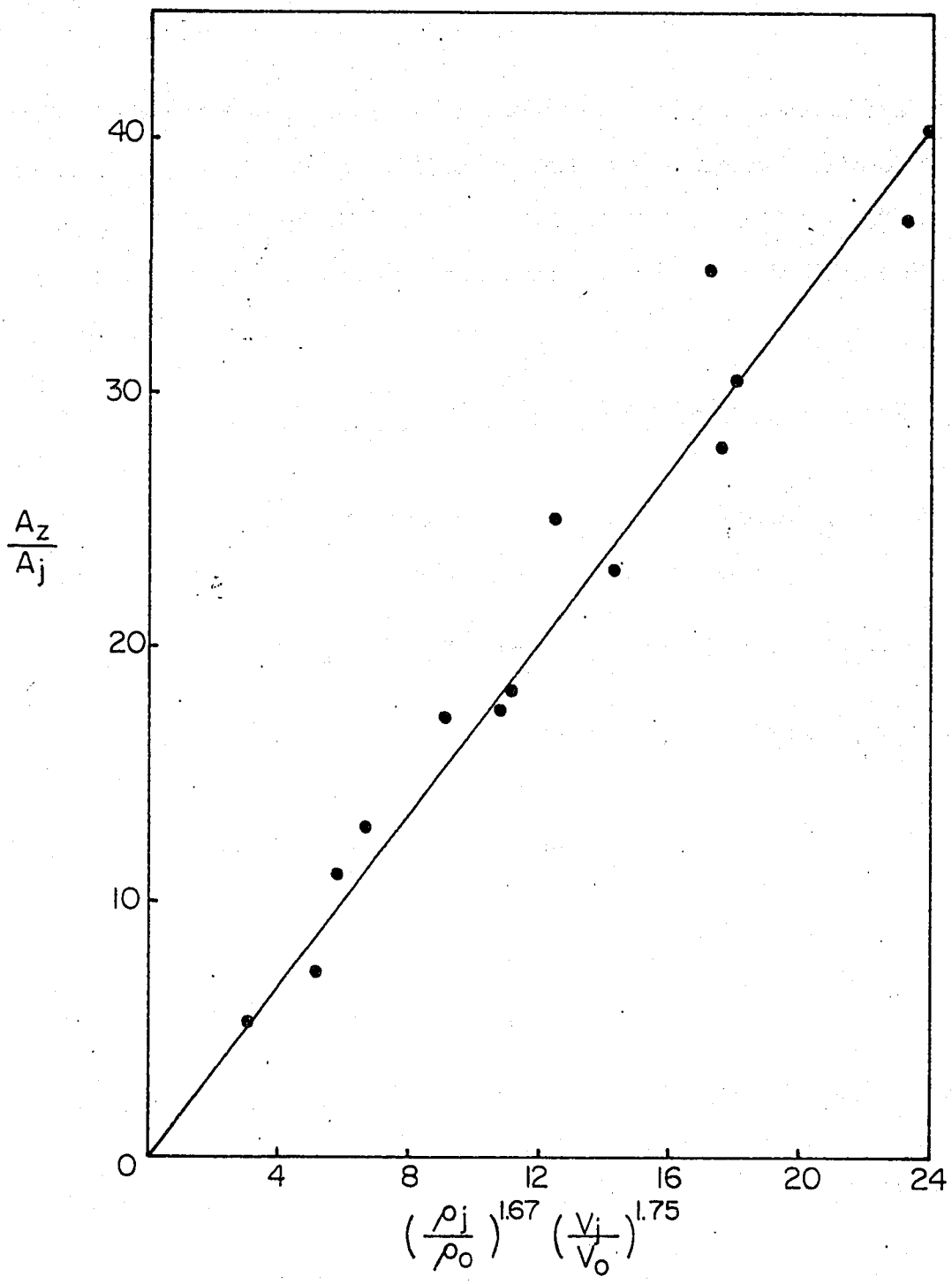
40
30
20
10
0
$\frac{A_z}{A_j}$
4
8
12
16
20
24
$\left(\frac{\rho_j}{\rho_o}\right)^{1.67}\left(\frac{V_j}{V_o}\right)^{1.75}$

Fig. 8

with jet Reynolds number could be observed. It is also seen that the ratio of the major axis to the minor axis of the stagnant elliptical zone is approximately 3:2 for almost all the cases. Hence in this analysis, knowing the area of the ellipse, one is able to find the length of the major and minor axes.

Correlation for the Angle of Inclination of the Major Axis of the Ellipse

The dimensional analysis gives the following relation for the angle of inclination of the major axis of the ellipse

$$\frac{\alpha}{45^\circ} = K \left(\frac{V_j}{V_0}\right)^a \left(\frac{\rho_j}{\rho_0}\right)^b \qquad (13)$$

where α = the angle of inclination of the major axis of the stagnant zone, in degree (see Fig. 5).

Equation (13) is represented by the relation

$$\alpha = 57.14 \left(\frac{V_j}{V_0}\right)^{-.927} \left(\frac{\rho_j}{\rho_0}\right)^{.933} \qquad (14)$$

which is obtained from the Figures 9 to 11.

Correlation for the Horizontal Distance from the Point of Injection, x

By similar dimensional analysis, the final correlation for this horizontal distance, from the point of injection, was found to be

$$\frac{x}{b_j} = 8.125 \left(\frac{V_j}{V_0}\right)^{-.82} \left(\frac{\rho_j}{\rho_0}\right)^{.65} \qquad (15)$$

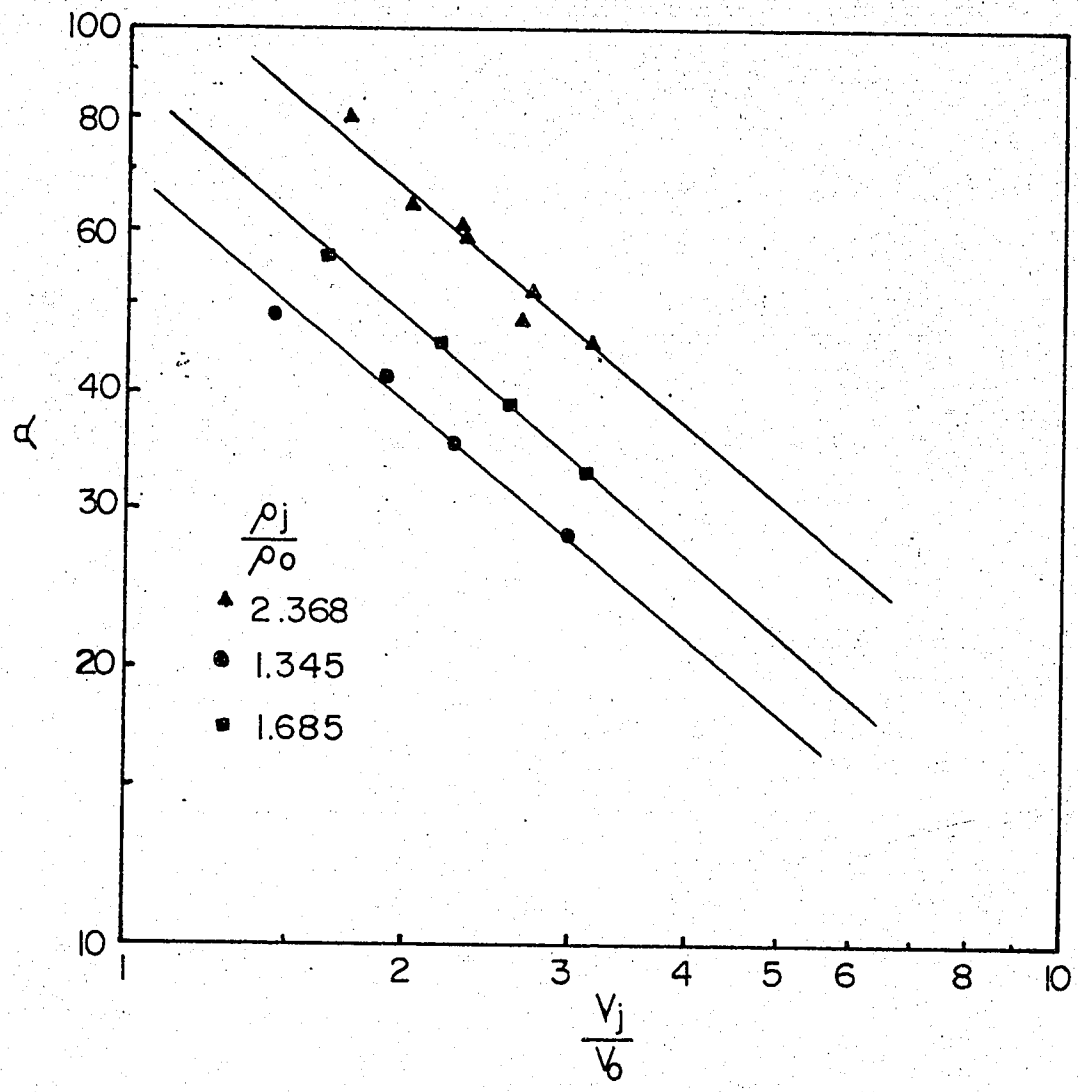

Fig. 9

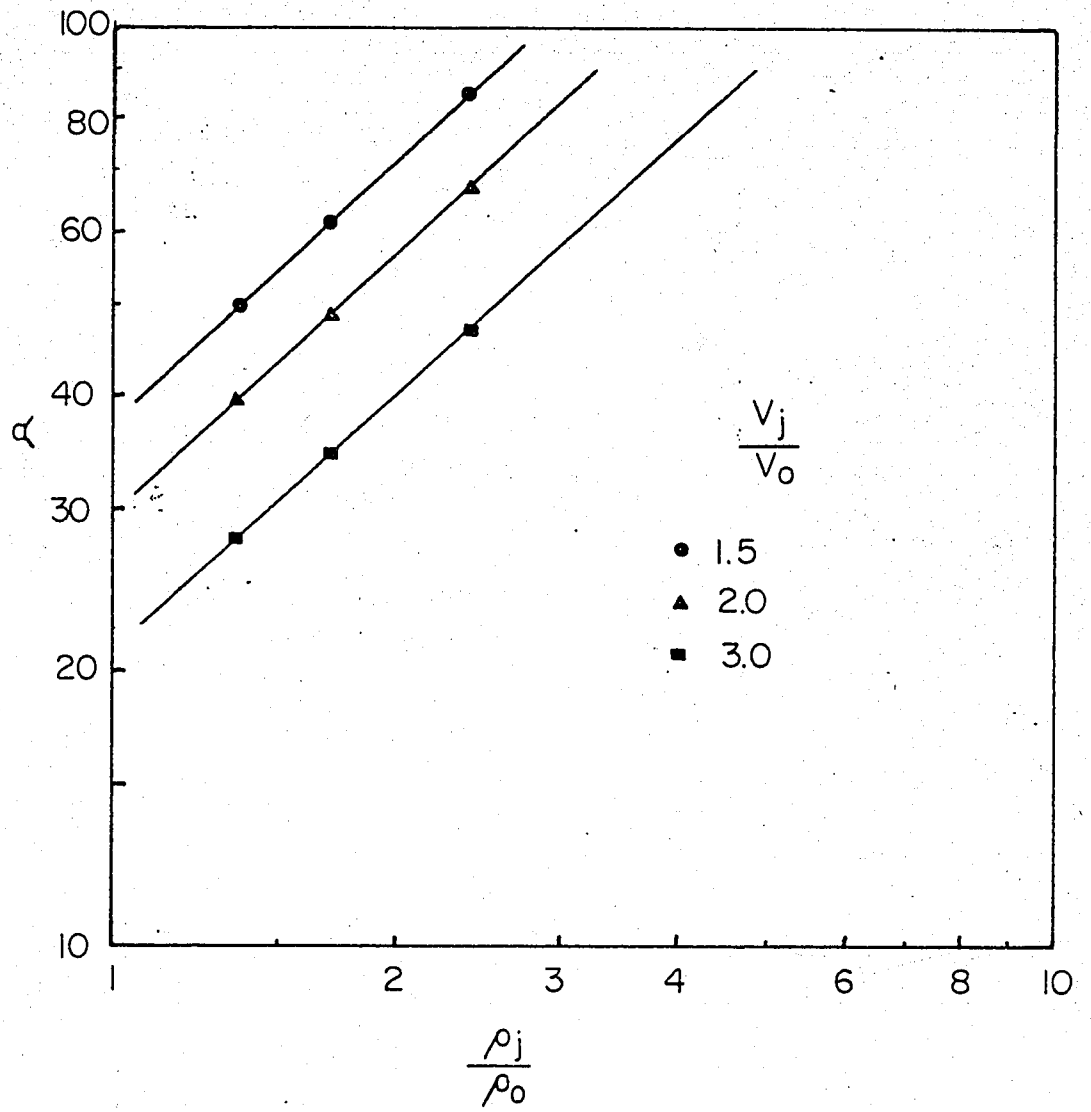
100
80
60
40
30
20
10
α
1
2
3
4
6
8
10
$\frac{\rho_j}{\rho_0}$
$\frac{V_j}{V_0}$
1.5
2.0
3.0

Fig. 10

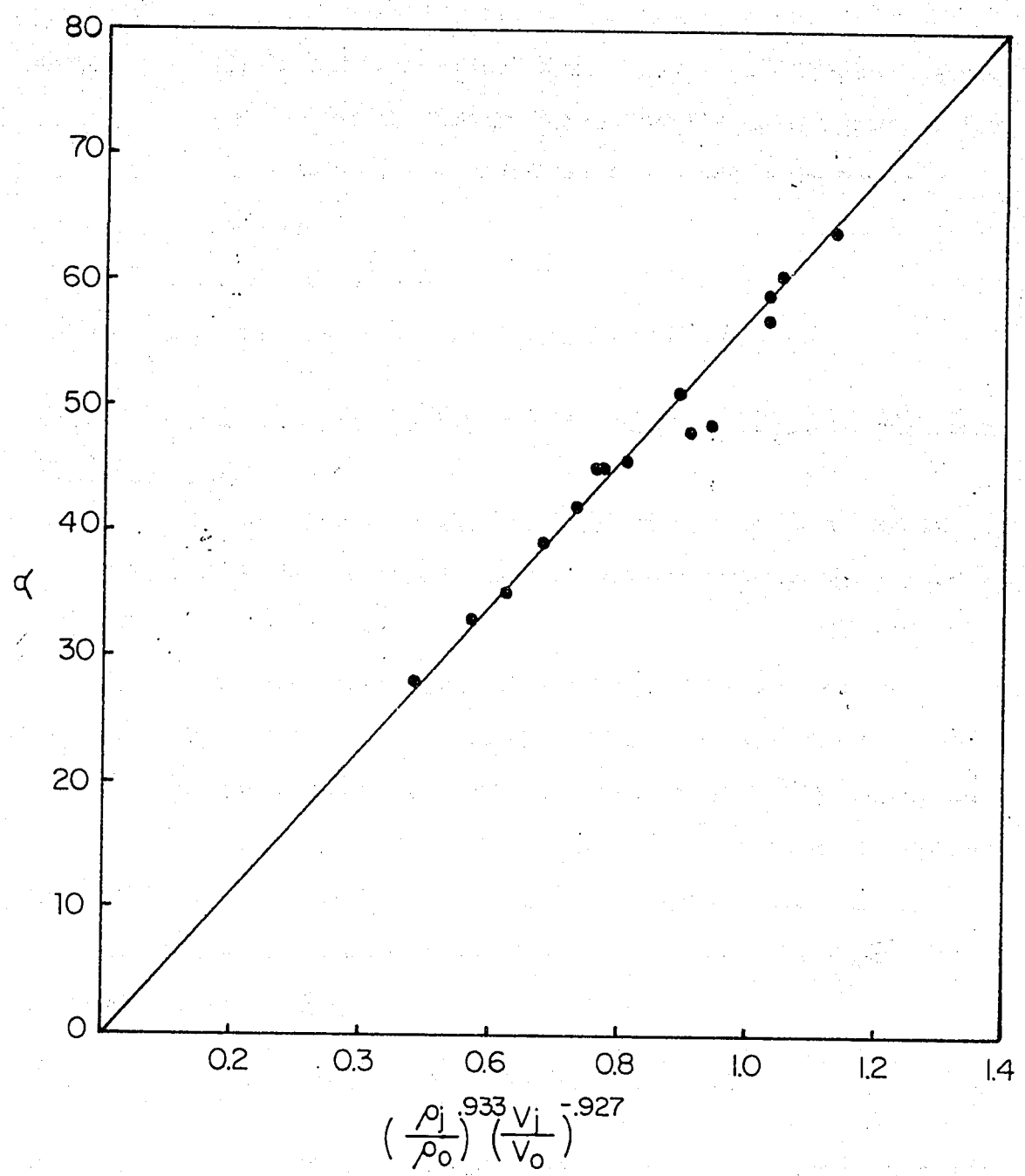
80
70
60
50
40
30
20
10
0
α
0.2
0.3
0.6
0.8
1.0
1.2
1.4
$\left(\frac{\rho_j}{\rho_0}\right)^{.933}\left(\frac{V_j}{V_0}\right)^{-.927}$

Fig. 11

where x = the horizontal distance from the point of injection to the point where the vertical line from the lowest point of the major axis of the elliptical zone touches the top wall (Figure 5)

b_j = width of the jet

The results of the analysis are given in Figures 12 to 14.

Correlation for the Vertical Distance of the Tip of the Major Axis From the Top Wall, y

In this case, no consistent trend of the data are obtained when y/b_j was plotted against V_j/V_0 with density ratio as the parameter (Fig. 15).

As another trial, y/b_j was plotted against the product $(\rho_j/\rho_0)(V_j/V_0)$ with b_j as the parameter (Fig. 16). Although the data shows a much better trend, the data seem to be a bit widely scattered.

Finally, the dimensionless factor $y/\sqrt{A_j}$ was plotted against $(\rho_j/\rho_0)(V_j/V_0)$ in Figure 17. This time all the data fall under a straight line within the acceptable limits of errors. The final correlation is therefore given by

$$y/\sqrt{A_j} = 1.458\ (\rho_j/\rho_0)\ (V_j/V_0) \qquad (16)$$

where y = the vertical distance of the lowest point of the major axis of the stagnant elliptical zone from the top wall.

The results of this analysis are shown in Figures 15 to 17.

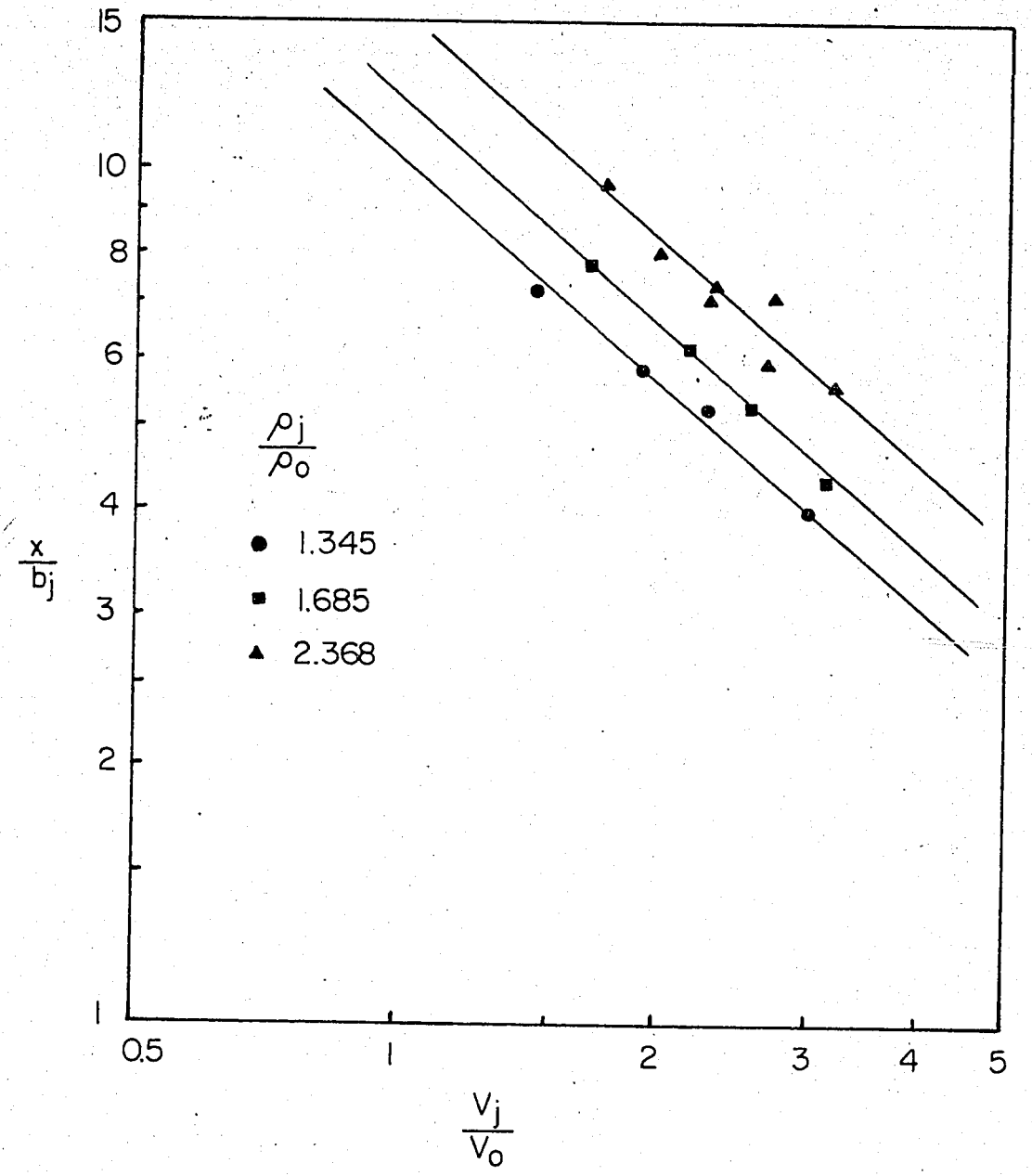

Fig. 12

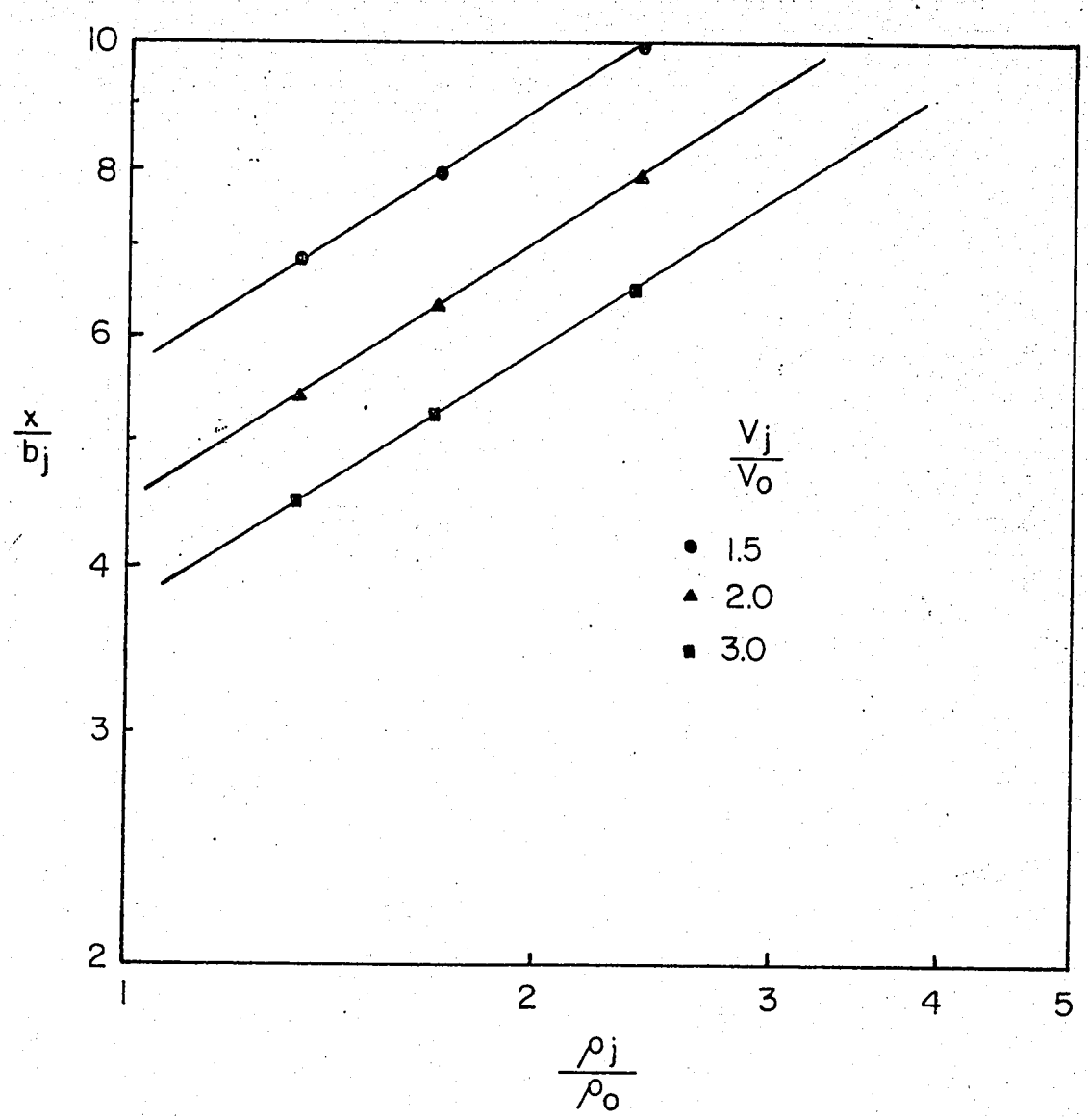

Fig. 13

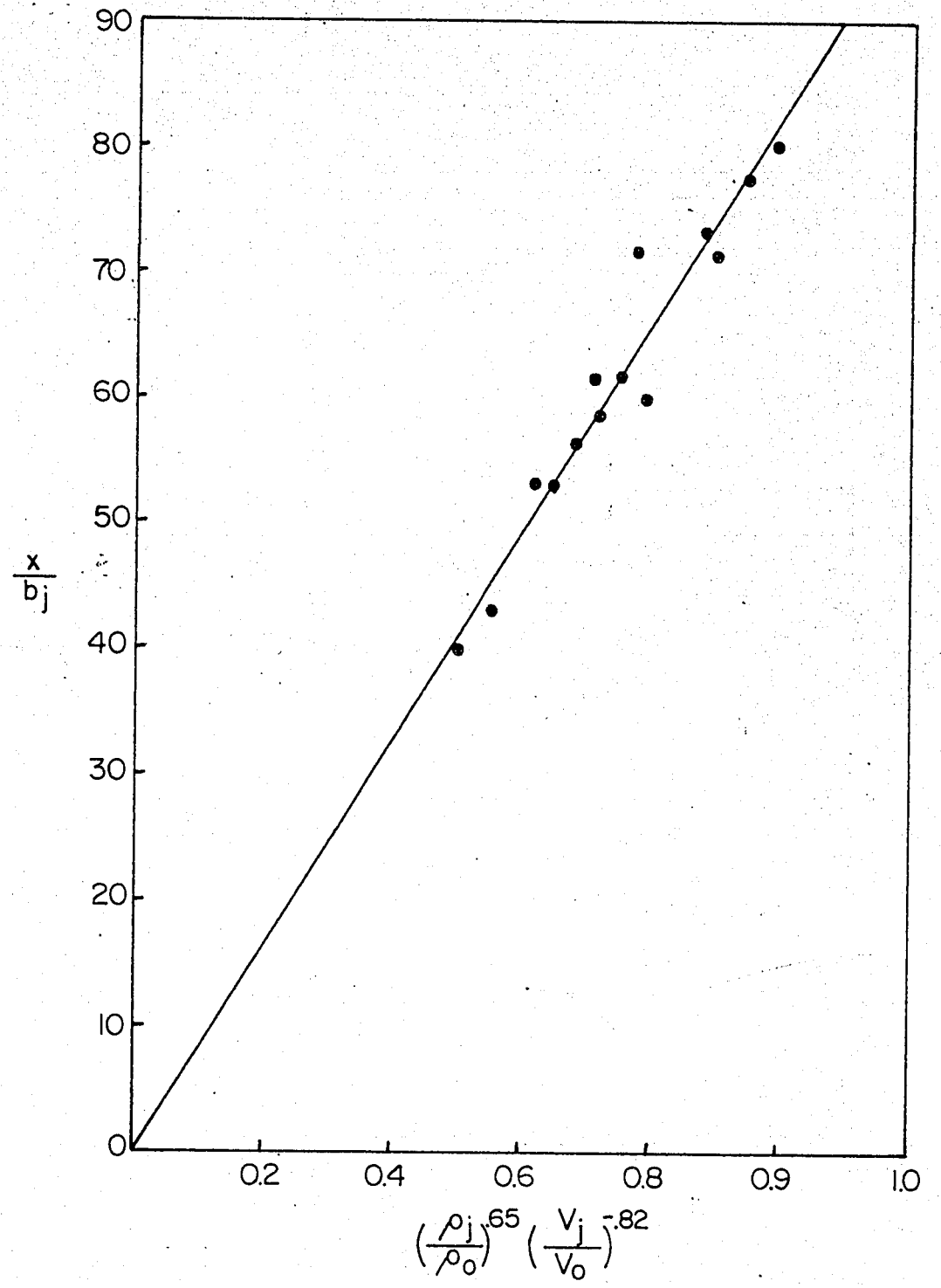
90
80
70
60
50
40
30
20
10
0
$\frac{x}{b_j}$
0.2
0.4
0.6
0.8
0.9
1.0
$\left(\frac{\rho_j}{\rho_o}\right)^{.65}\left(\frac{V_j}{V_o}\right)^{-.82}$

Fig. 14

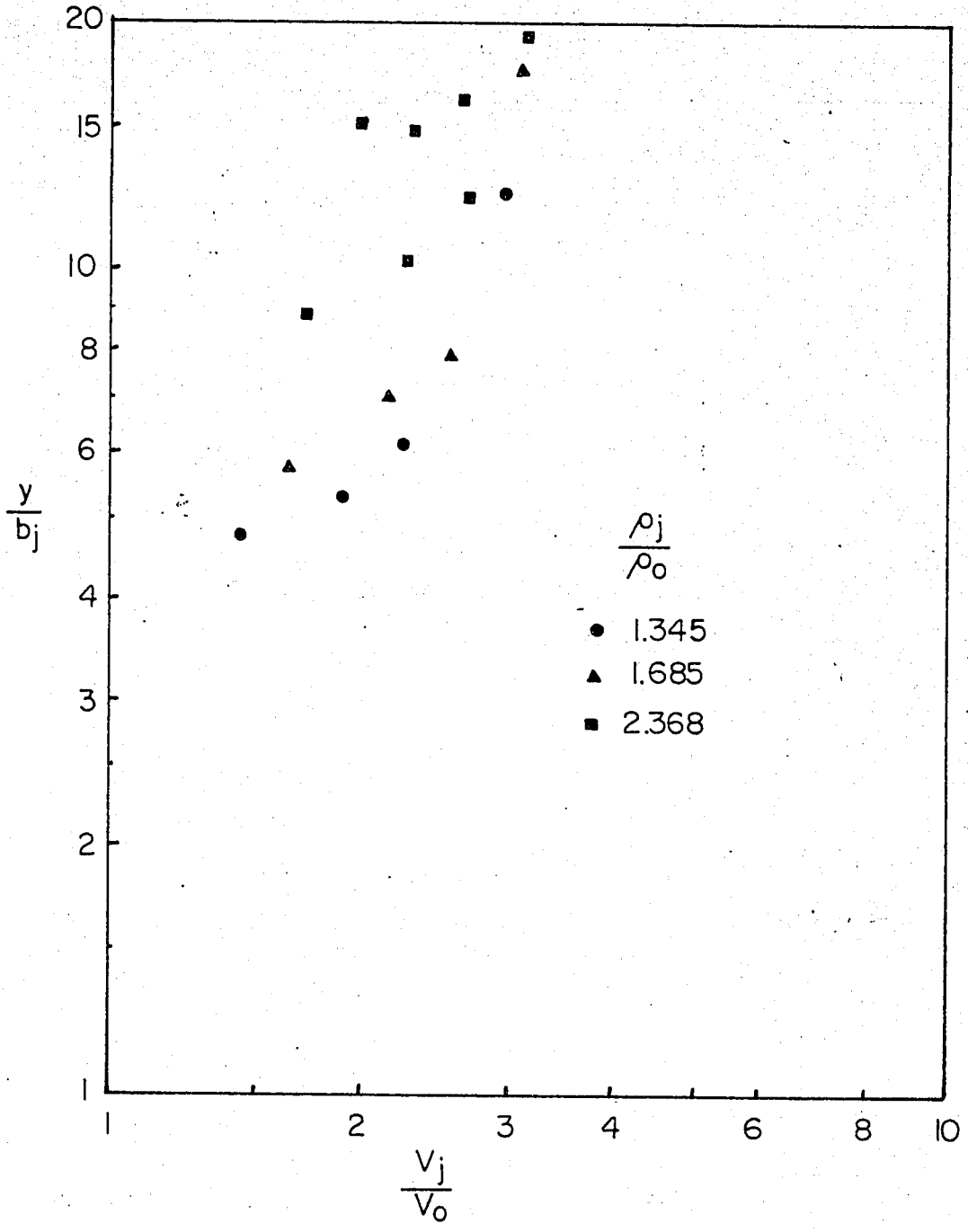

Fig. 15

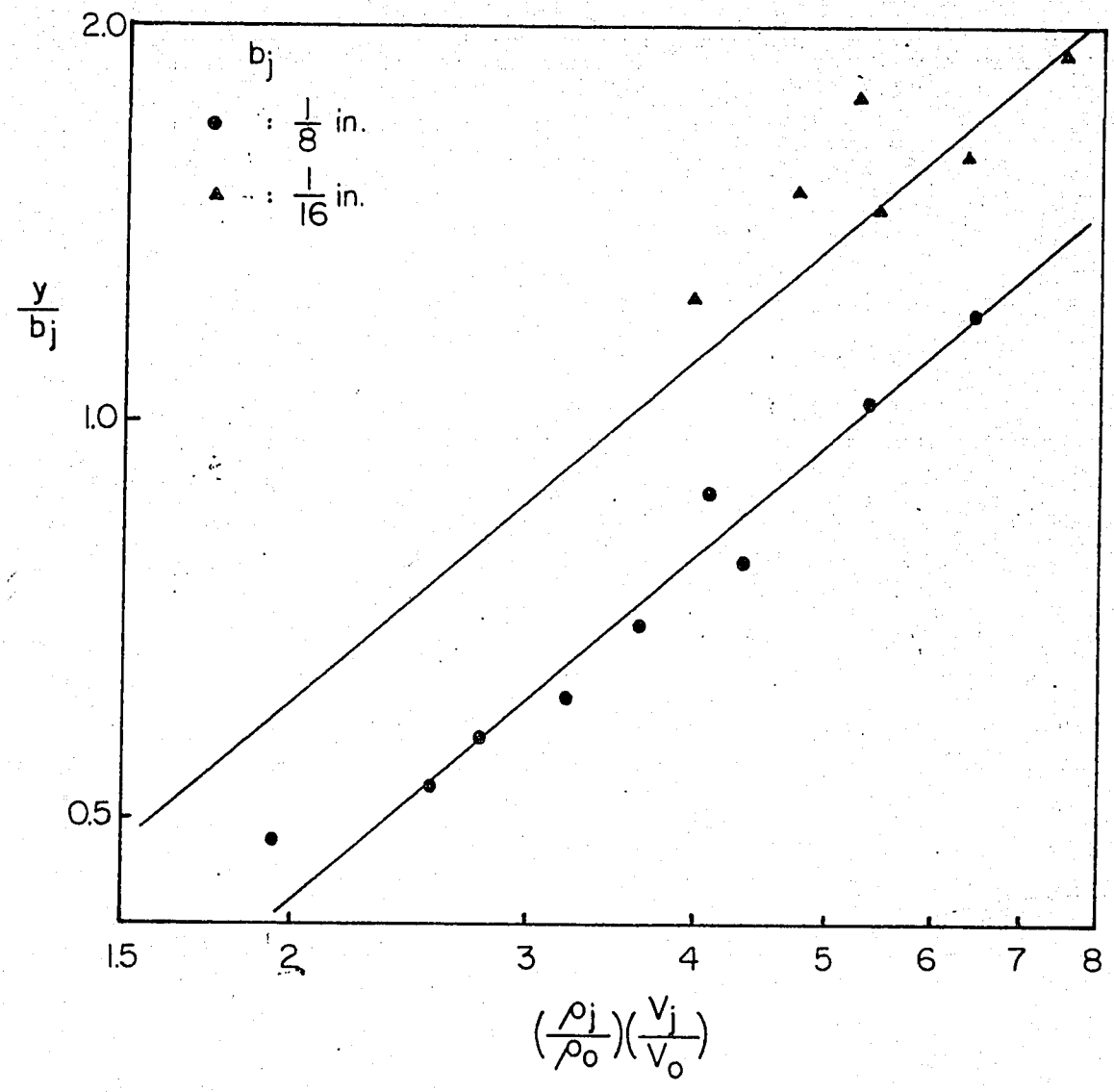
2.0
1.0
0.5
b_j
● : $\frac{1}{8}$ in.
▲ : $\frac{1}{16}$ in.
$\frac{y}{b_j}$
1.5
2
3
4
5
6
7
8
$(\frac{\rho_j}{\rho_0})(\frac{V_j}{V_0})$

Fig. 16

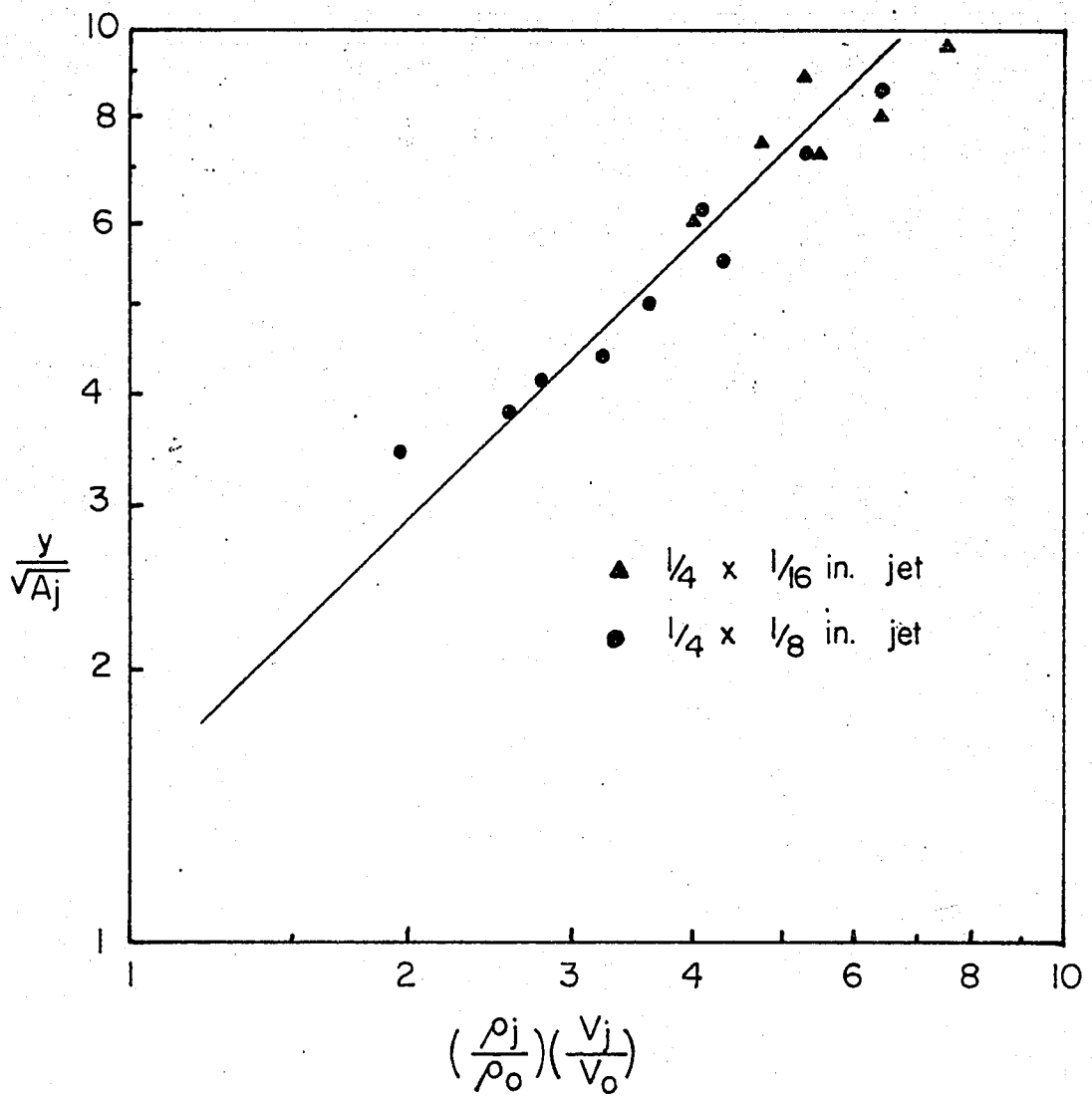

Fig. 17

TABLE I

Jet Dimension	Main Velocity V_0 F.P.S.	Jet Pressure P_j psig.	$\frac{\rho_j}{\rho_0}$	Jet Velocity V_j F.P.S.	Stagnant Zone area A_z sq. in.	$\frac{A_z}{A_j}$	$\frac{V_j}{V_0}$	x in.	y in.	Angle of inclination α degree
1/4" by 1/8"	132.5	5	1.345	300	.40	12.85	2.26	.66	.77	35
"	"	10	1.685	340	.78	24.96	2.56	.66	.98	39
"	"	15	2.02	354	1.08	34.72	2.67	.77	1.14	45
"	"	20	2.368	358	1.26	40.28	2.7	.89	1.52	51
"	208	5	1.345	300	.16	5.27	1.44	.89	.60	48.5
"	"	10	1.685	340	.35	11.11	1.64	.97	.72	57
"	"	20	2.368	358	.54	17.36	1.72	1.21	1.10	81
"	"	30	3.05	362	.87	27.78	1.74	1.37	1.27	90
"	158	5	1.345	300	.22	7.23	1.9	.73	.66	41.5
"	"	10	1.685	340	.54	17.36	2.15	.77	.87	45.5
"	"	20	2.368	358	.87	27.78	2.26	.89	1.29	60.5

....cont.

TABLE I (continued)

Jet Dimension	Main Velocity V_0 F.P.S.	Jet Pressure P_j psig	$\frac{\rho_j}{\rho_0}$	Jet Velocity V_j F.P.S.	Stagnant Zone area A_z sq. in.	$\frac{A_z}{A_j}$	$\frac{V_j}{V_0}$	x in.	y in.	Angle of inclination α degree
1/4" by 1/16"	182	20	2.368	419	.48	30.55	2.3	.46	.92	59
"	132.5	20	2.368	419	.89	56.86	3.16	.35	1.21	45
"	"	10	1.685	413	.54	34.72	3.11	.27	1.10	33
"	"	5	1.345	392	.28	18.01	2.96	.25	.77	28
"	158	20	2.368	419	.57	36.67	2.65	.37	1.00	47.75
"	208	20	2.368	419	.35	22.22	2.01	.50	.94	64

The discussions of the stagnant elliptical zone so far have been related to the central vertical plane ABCD. However, for a complete understanding of the stagnant zone, one should consider this zone as a volume instead of as an area. Hence, one should also be interested to see whether this stagnant zone is also present at the vertical plane away from the centre. Point velocities in the vertical plane at different distances away from the centre of the duct width are noted from the chart readings, and plotted in the Figures 18 to 21 for several different cases. From these figures, it is noted that the same type of stagnant elliptical zone is present at other vertical planes away from the centre point of the duct width, up to a certain distance away from the centre of the duct width.

It can also be observed from these figures that, for any particular case (the jet dimension and the main velocity remaining the same), the stagnant zone in the plane ABCD (Figure 3) exists up to greater distances away from the centre of the duct with higher jet pressures. Thus when the jet pressure is 10 pounds per square inch (for the 1/4" by 1/8" jet with a main velocity of 132.5 feet per second) the stagnant zone at the plane ABCD exists up to a distance of 3/8" for both sides from the centre of the duct (Figure 19). Whereas, when the jet pressure is 20 pounds per square inch for the same case, the stagnant zone exists up to 1/2" from the centre point of the duct (Figure 18). The findings about the width of the stagnant zone, drawn from the data may be summarized as follows.

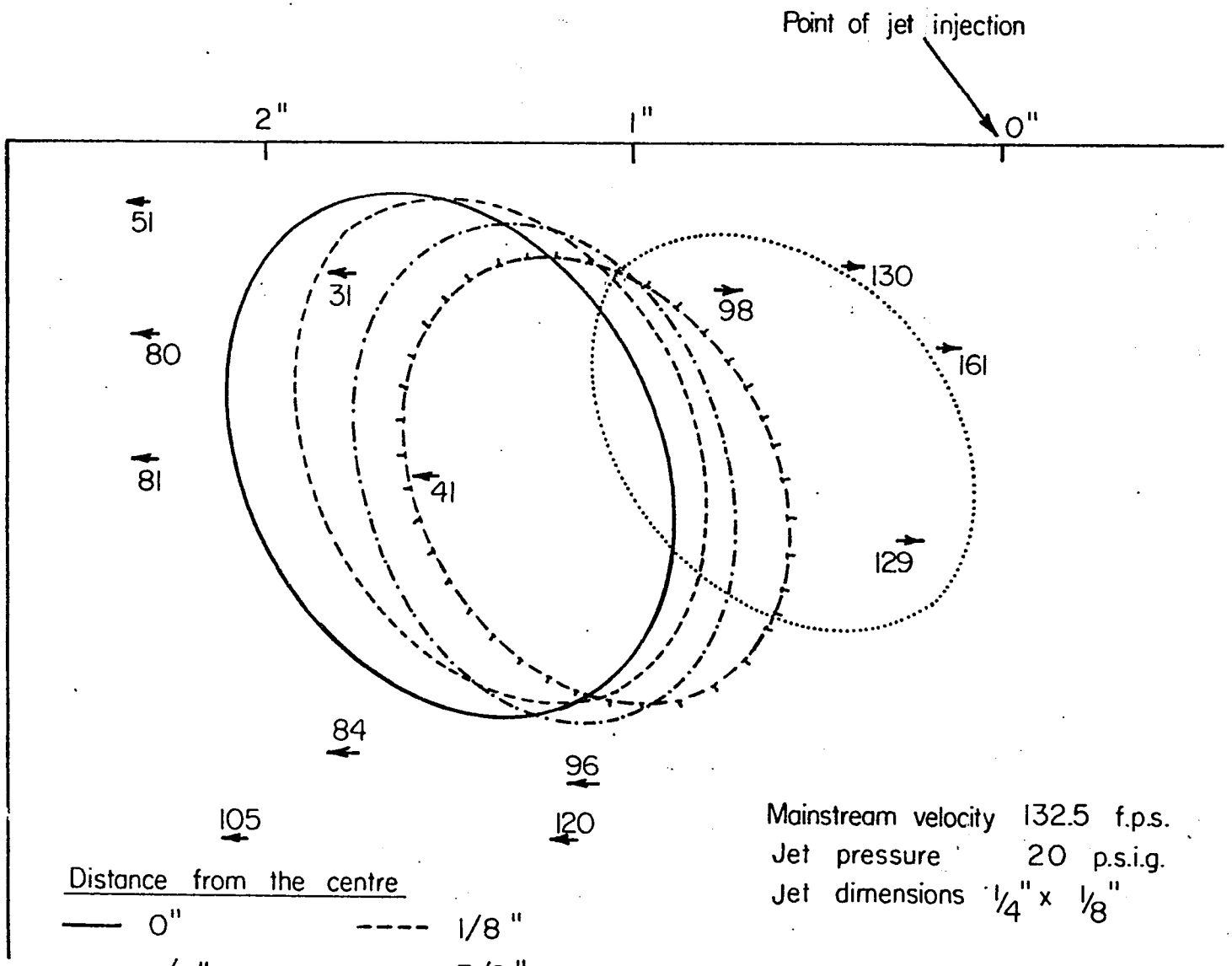

Fig. 18. Stagnant zones of recirculation in the plane A-B-C-D (arrows indicate the point velocities at the centre of the duct width)

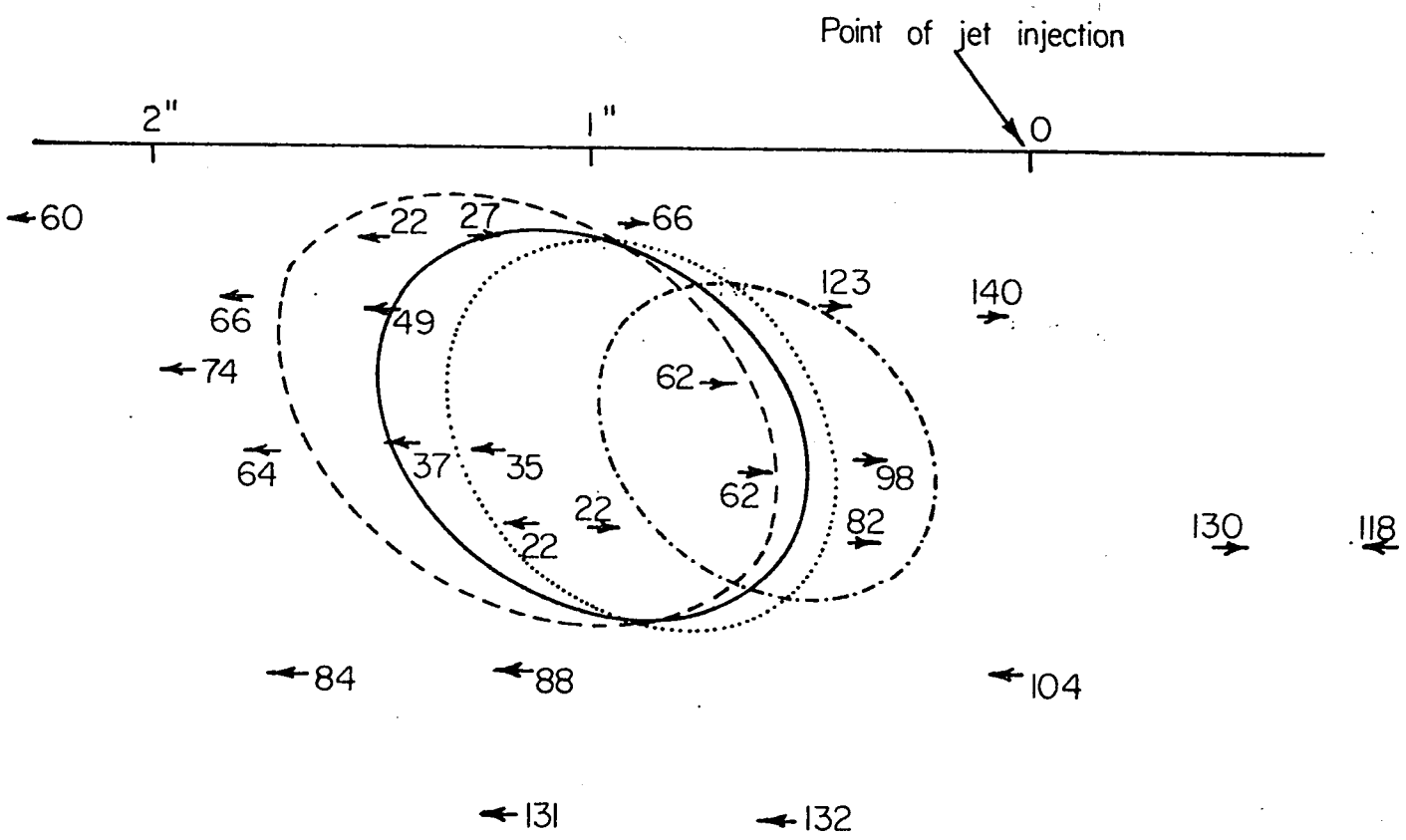

Distance from the centre

----- : 0" ——— : 1/8"

..... : 1/4" -.-.-.- : 3/8"

Mainstream velocity : 132.5 f.p.s

Jet pressure : 10 p.s.i.g.

Jet dimensions : 1/4 x 1/8 in.

Fig. 19. Stagnant zones of recirculation in the plane A-B-C-D (arrows indicate the point velocities at the centre of the duct width)

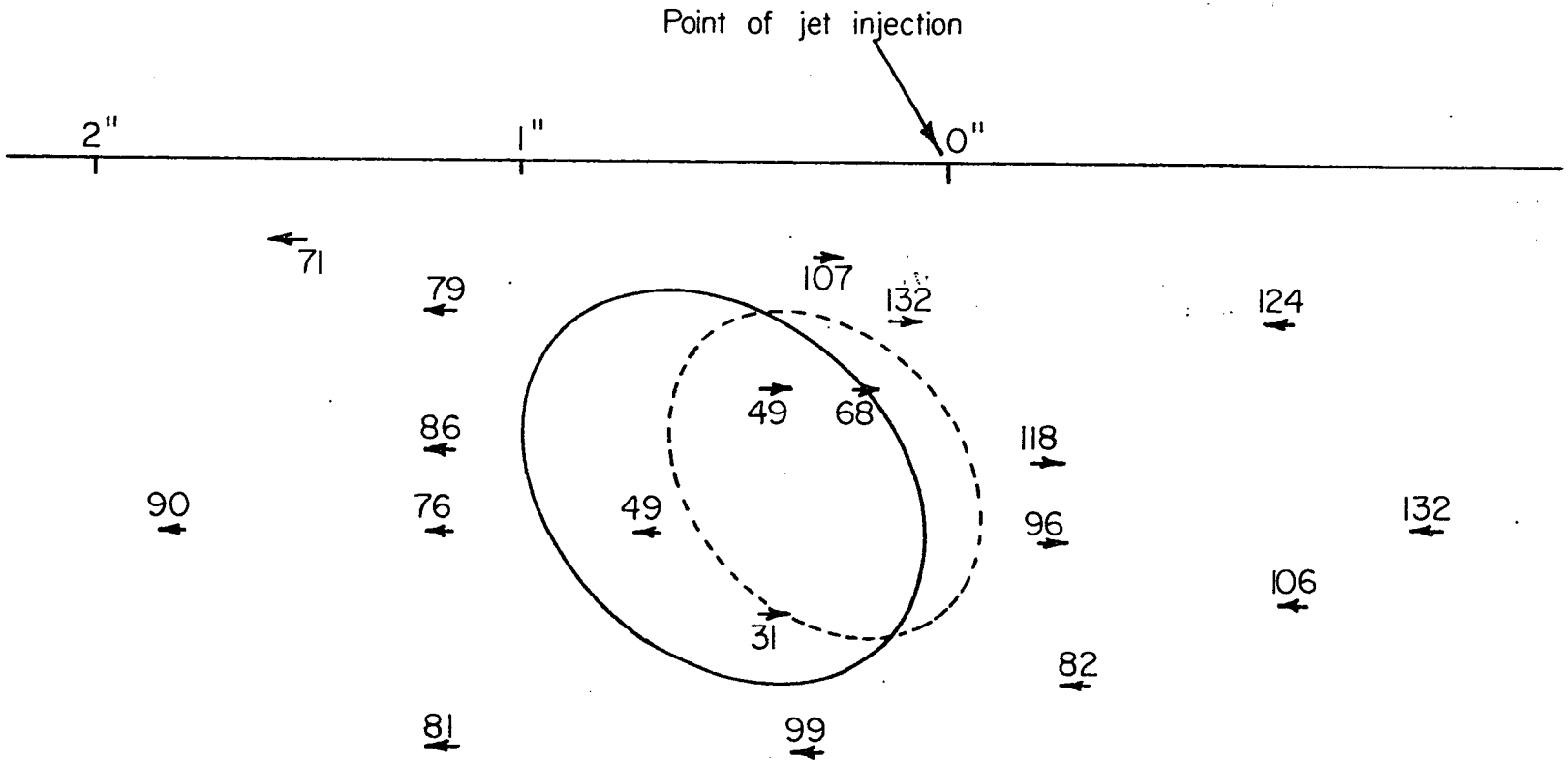

Fig. 20. Stagnant zones of recirculation in the plane A-B-C-D (arrows indicate the point velocities at the centre of the duct width)

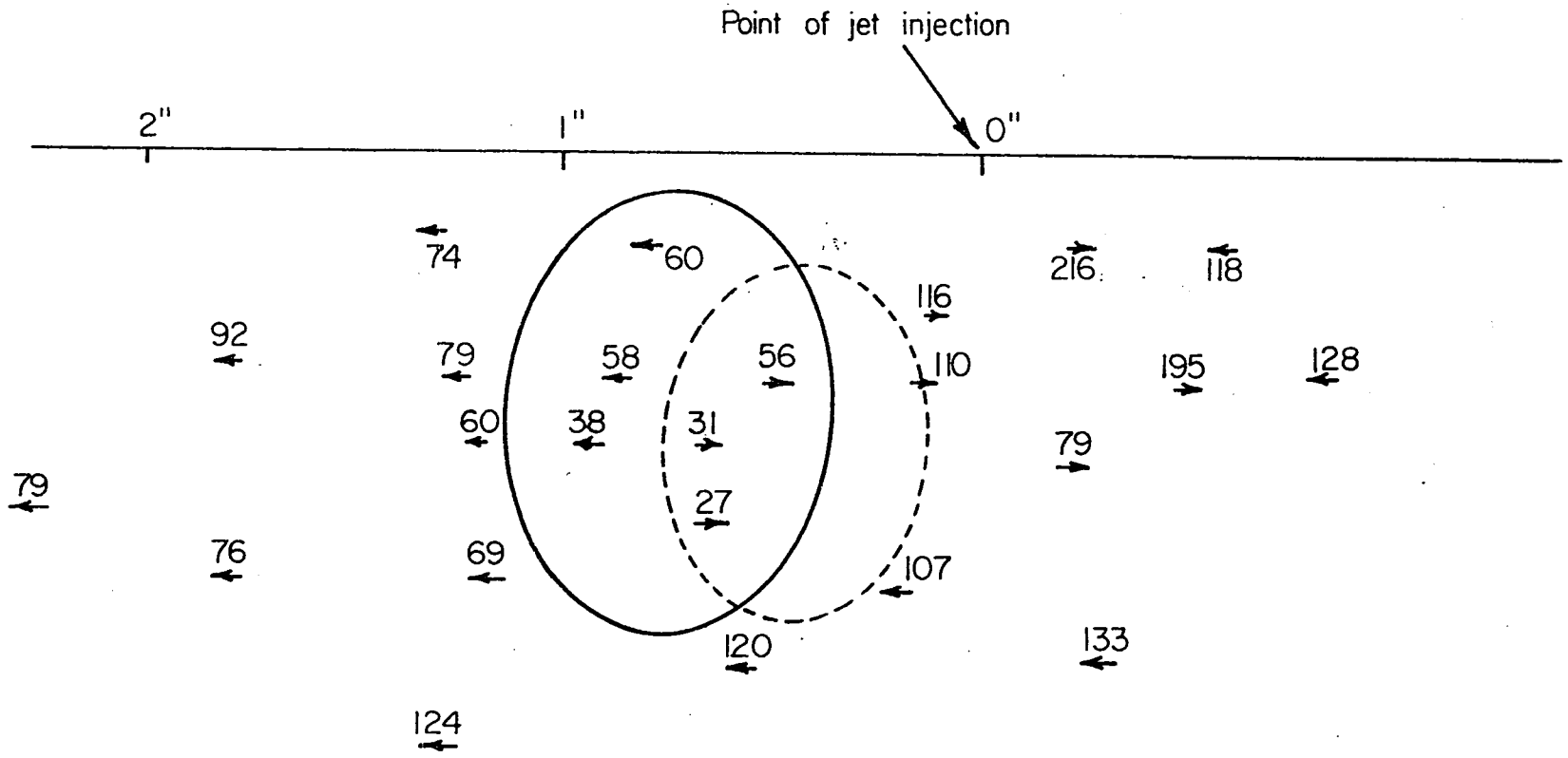

Distance from the centre

——— 0"

----- 1/8"

Mainstream velocity 132.5 f.p.s.

Jet pressure 10 p.s.i.g.

Jet dimensions 1/4 x 1/16 in.

Jet orientation ▭ ←

Fig. 21. Stagnant zone of recirculation in the plane A-B-C-D (arrows indicate the point velocities at the centre of the duct width)

The width of the stagnant zone depends primarily on the mass velocity of the jet, and not on the orientation of the jet (whether the long or short side of the jet is against the direction of the main flow) with regard to the main flow. Thus, no significant difference in the width of the stagnant zones was obtained with the 1/4" by 1/16" jet with its two different cases of orientation (see Figures 20 and 21). Other things remaining the same, the width of the stagnant zone with 1/4" by 1/8" is greater than that with 1/4" by 1/16" (Figures 20 and 19). However, it is to be remembered that the above discussion about the width of the stagnant zone is valid within the experimental range of variables investigated. The observations regarding the width of the stagnant recirculated zone, from the Figures 18 to 21, are tabulated below.

TABLE II

Jet Dimension	Main Stream Velocity F.P.S.	Orientation of the jet	Jet Pressure psig	Total width of the Stagnant zone in inch	Representative Figure
1/4" x 1/8"	132.5	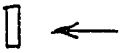	20	1	18
1/4" x 1/8"	"	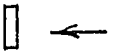	10	3/4	19
1/4" x 1/16"	"	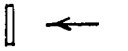	10	1/4	20
1/4" x 1/16"	"	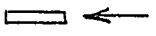	10	1/4	21

In a somewhat similar type of investigation, Bertin and Salmon (37) drew an analogy between the case of a two-dimensional obstacle and the slot jet. From their experimental observations they obtained a loop

of null velocities in the wake of the injector, and concluded that the area within this null velocities loop is the zone of recirculation of the fluid flow.

Figure 4 is a vector diagram showing the point velocities at different positions in the plane ABCD. It may be pointed out here that in the wake drawn on this figure a reverse flow can be clearly seen. Also a loop of null velocities can be drawn in the wake of the injector as shown by the line in Figure 4.

It is believed, however, that the analogy drawn between a slot jet and metal baffle is somewhat misleading. A metal baffle is a solid rigid object whose shape and position remain fixed irrespective of the main stream flow properties. On the other hand, a fluid jet is quite flexible. Here is the case of two fluid streams, both of which will be altered from their original characteristics after their mutual collision in the duct. Thus the penetration of the jet in the main stream is as much dependent on the main stream velocity as it is on the jet pressure. In contrast to this, the protrusion of the metal baffle in the duct and hence in the main stream fluid flow stays unaltered. The physical systems in the two cases are very much different from one another.

Bertin and Salmon (37) also observed that if the slot jet is inclined to 45° against the main flow, the reverse zone enlarged considerably in comparison to the reverse zone in the case of perpendicular injection under identical conditions. In the case of a metal baffle, if the dimensions remain the same, the size of the reverse zone should

not alter much with the angle of inclination of the baffle. Thus this is another point against the disputed analogy.

Figure 22 shows the breakdown of the velocities measured at different points along the length of the flow lines in the case of transverse jet injection perpendicular to the axis of the mainstream flow, as given by Bertin and Salmon (37). Similar velocity profiles drawn from the data of the present work are shown in Figures 23 to 26 for four different cases of jet injection at an angle of 45° to the axis of the mainstream flow.

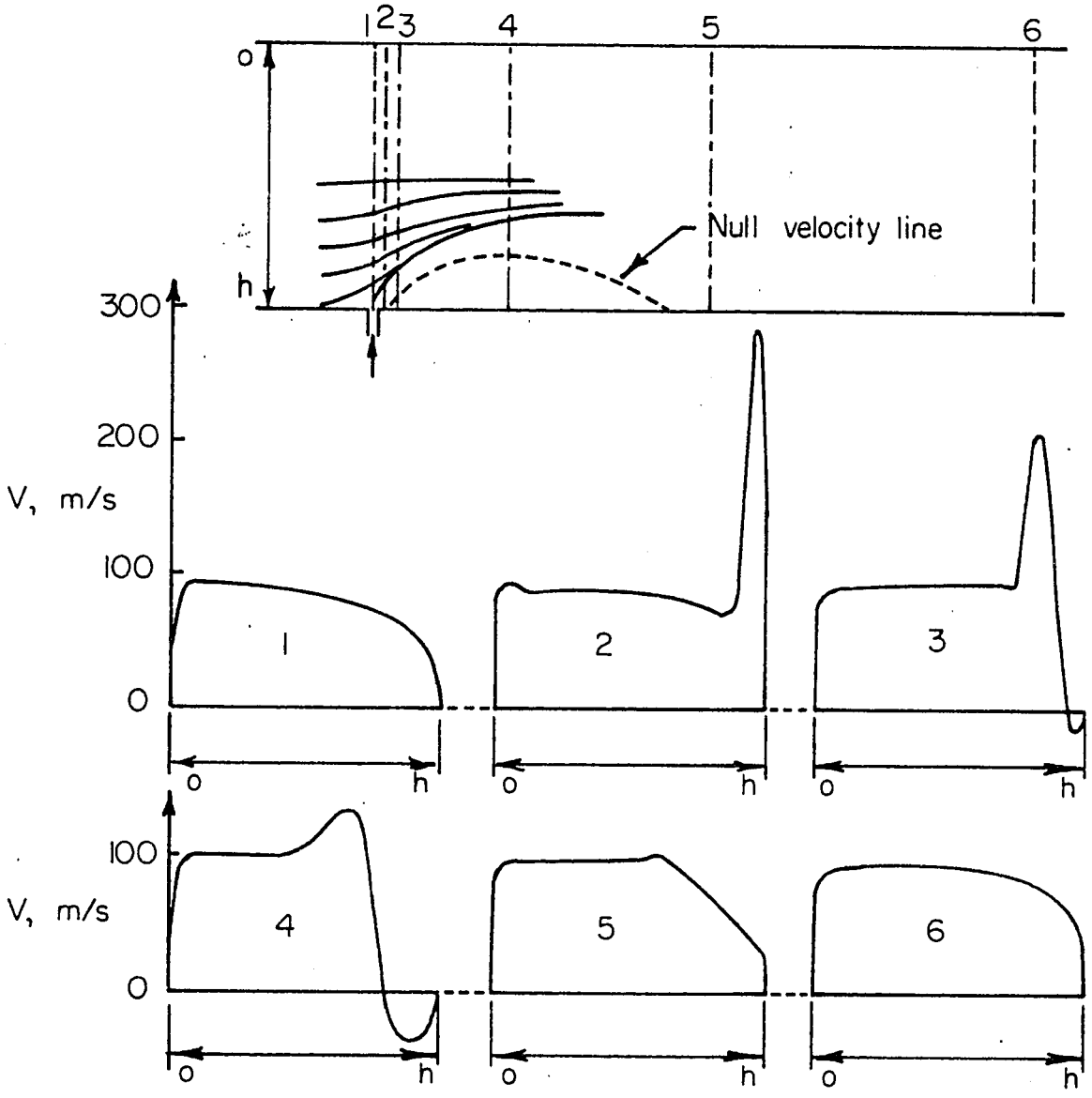

Fig. 22. Velocities at different points along the length of the flow lines (as given by Bertin and Salmon)

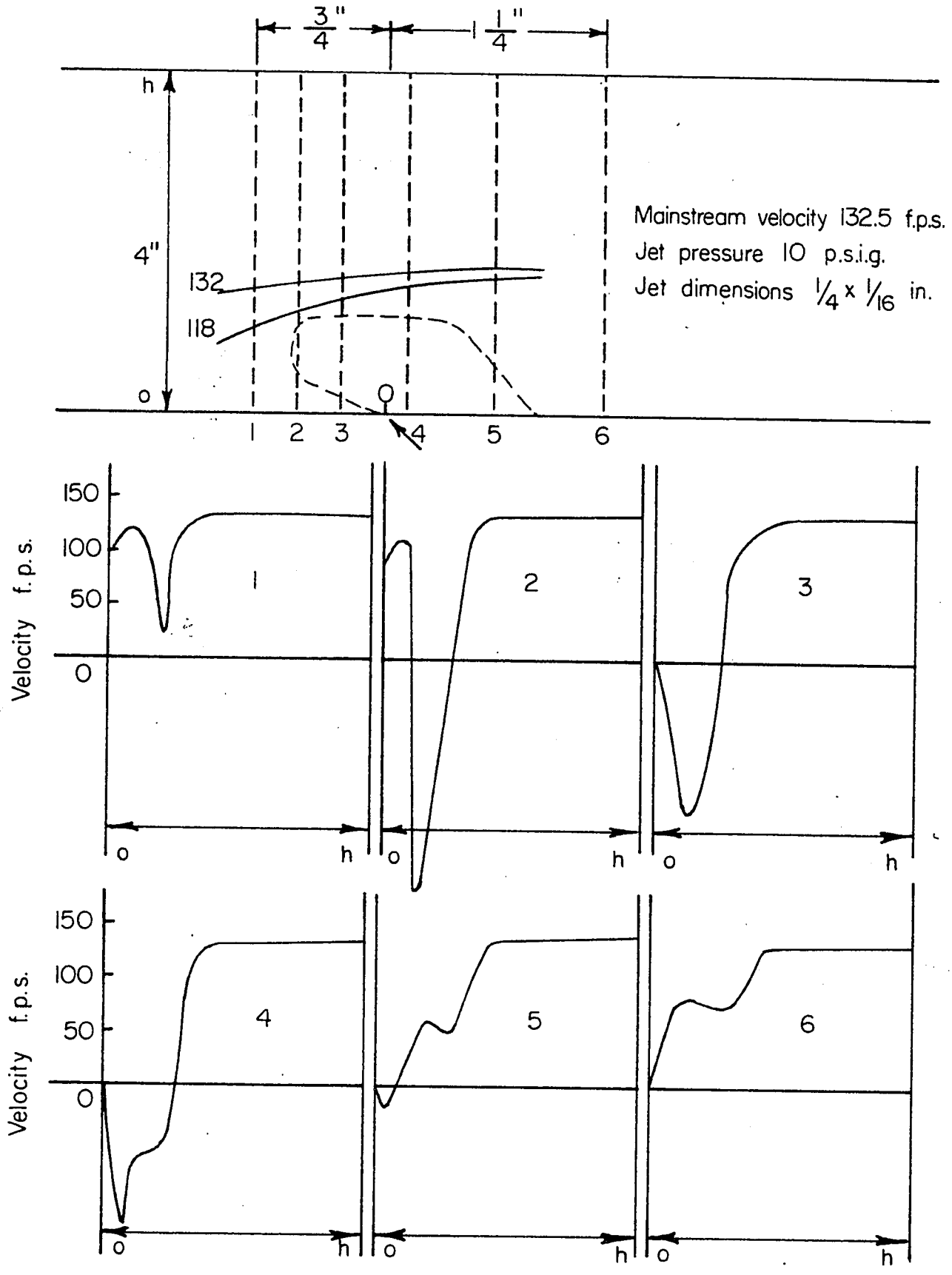

Fig. 23. Velocities at different points along the length of the flow lines

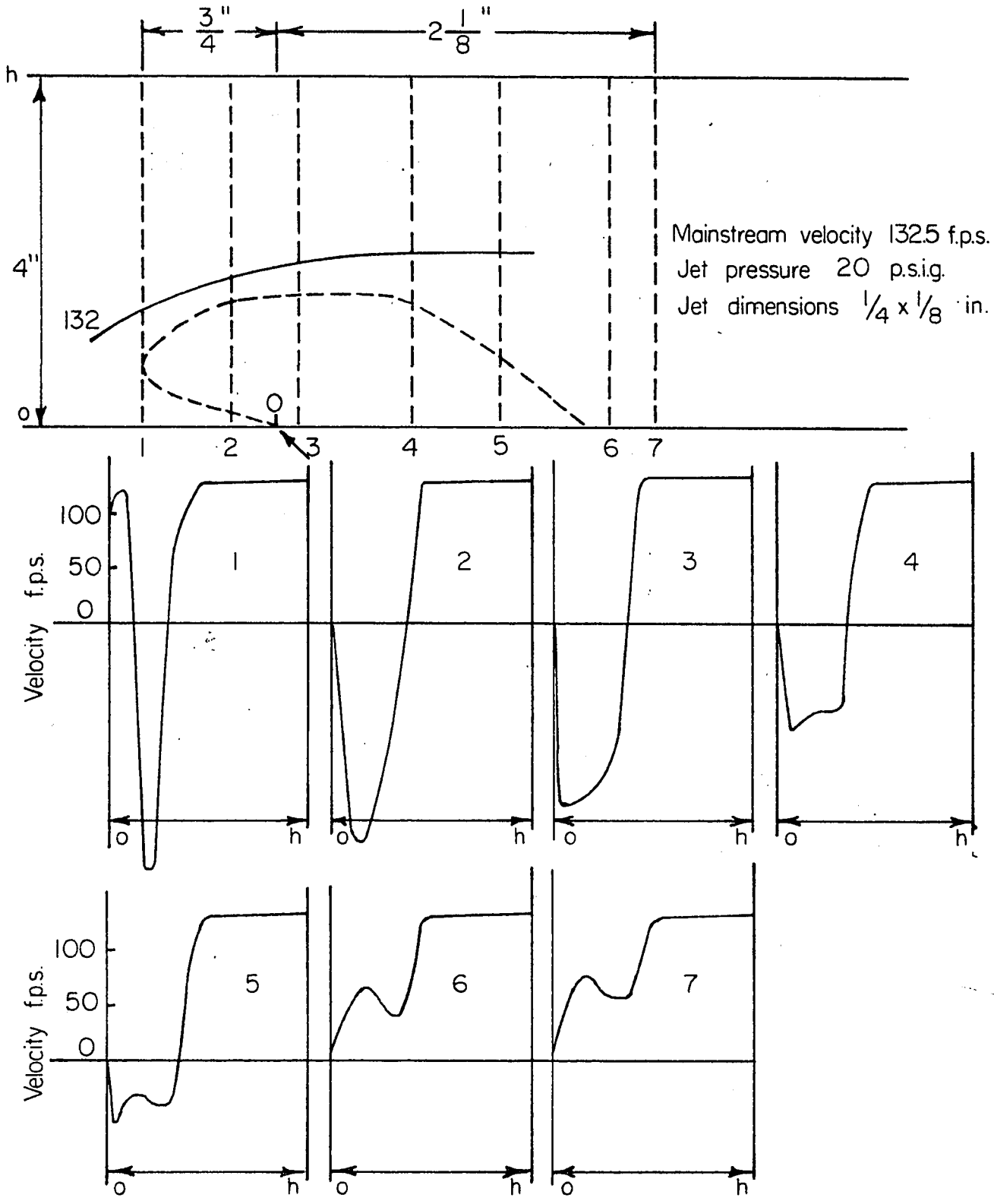

Fig. 24. Velocities at different points along the length of the flow lines

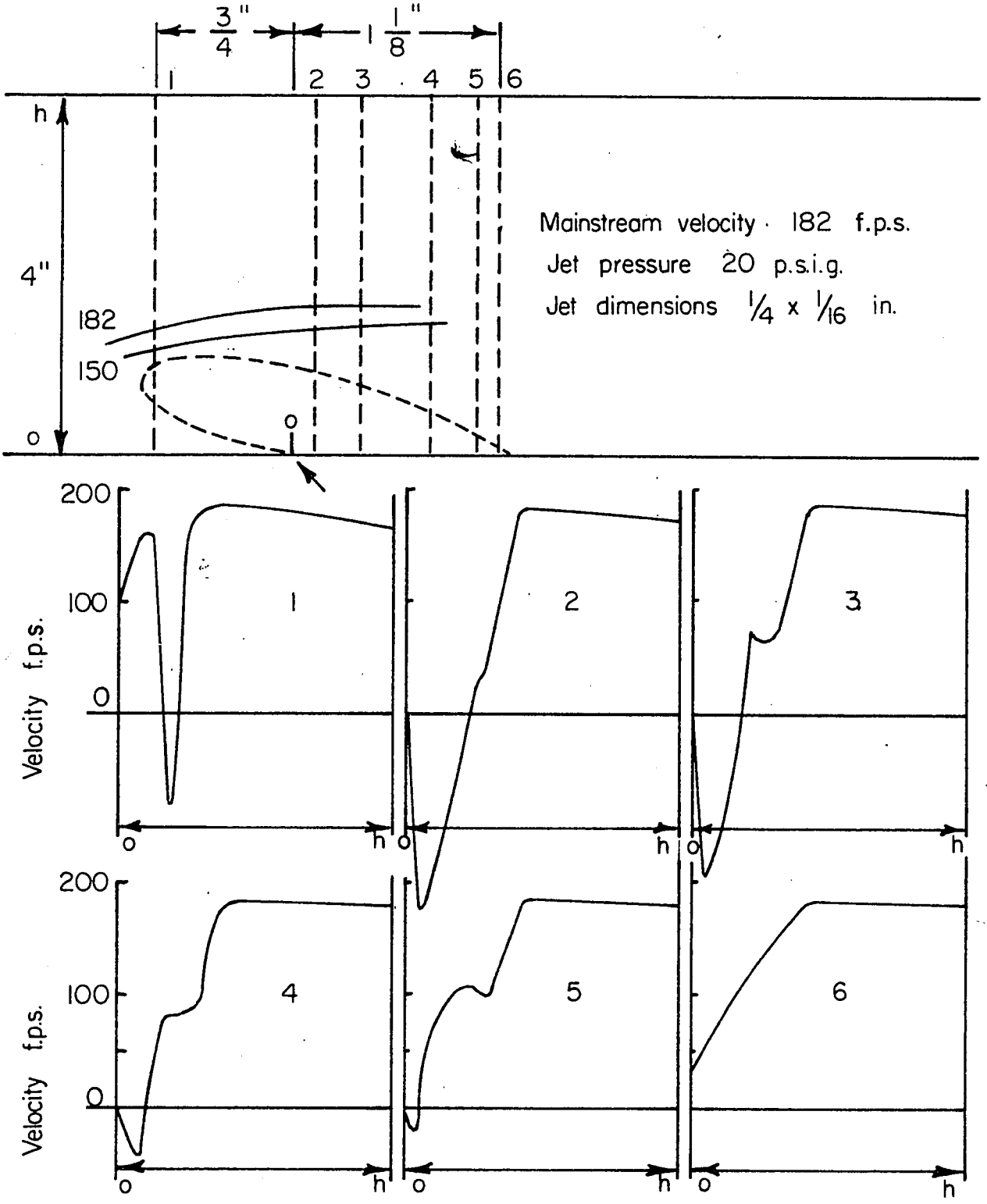

Fig. 25. Velocities at different points along the length of the flow lines

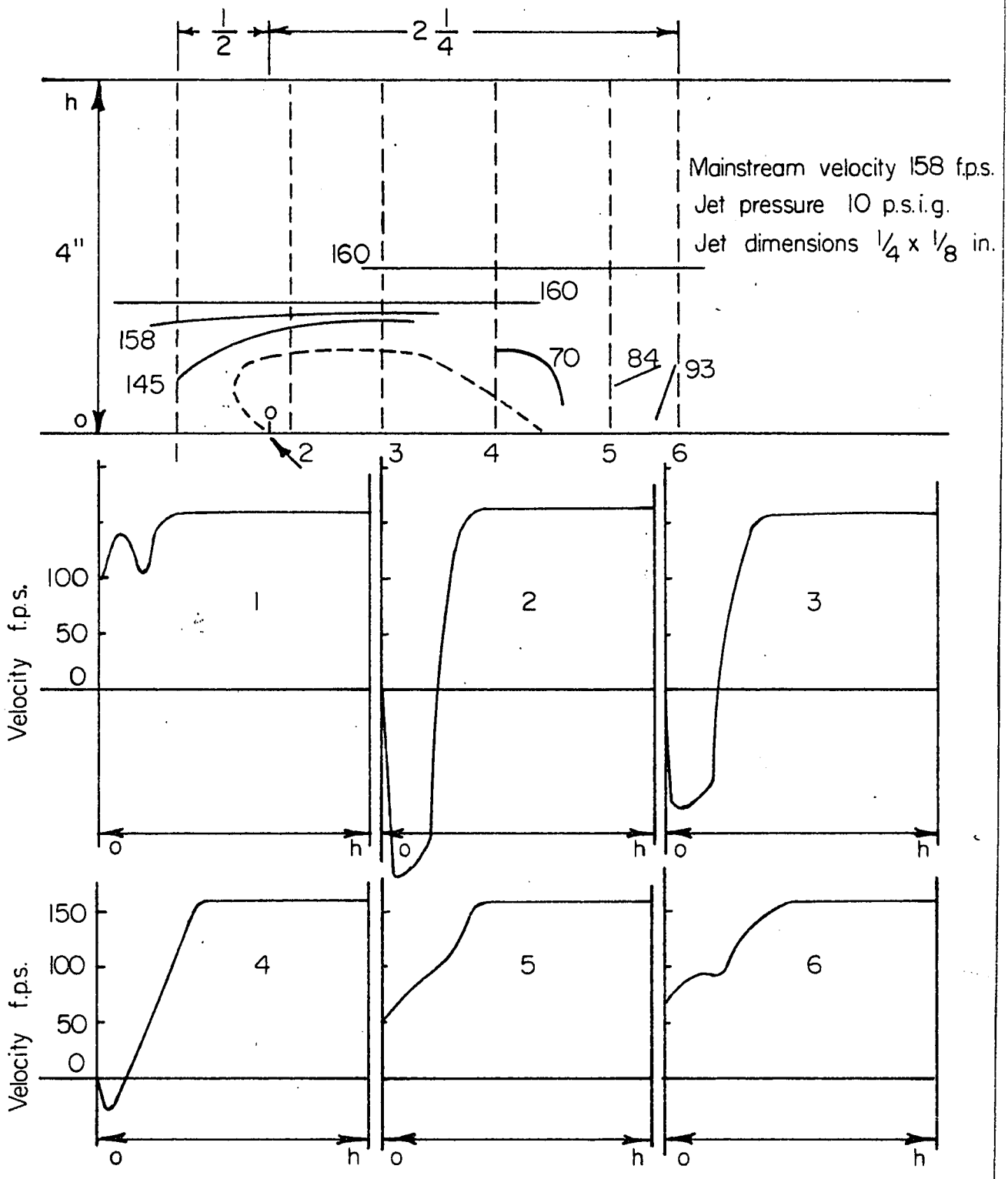

Fig. 26. Velocities at different points along the length of the flow lines

If the velocity profiles in the following stations, namely,

a) immediately downstream of the jet injector

b) at the centre of the null velocity region (shown by the dotted lines in the Figures 22 to 26)

c) near the downstream end of the null velocity loop

are compared, then two distinct differences are noticed between Bertin and Salmon's (37) results and the results of present investigation. They are:

1) the velocities of the reversal flow in the present experiment are rather high compared to the data of Bertin and Salmon (37).

2) The velocity gradients around the null velocity line in the stations of the downstream half of the null velocity loop (stations 4, 5 and 6 in Figure 23) are very much less than the velocity gradients elsewhere in the same plane; this trend is not noticeable from Bertin and Salmon's (37) results (Fig. 22).

The differences between the results of these two nearly similar experiments (Bertin and Salmon (37), and the presenk work) may well be due to the fact that the previous workers (37) used total pressure probe rake directly into the recirculation zone which could disturb the flow considerably. The change in the velocity gradient as indicated in point (2) above, in the present experiment, could be explained by the interpretation that around these points the flow direction takes its turn and thereby an elliptical zone of recirculation is created, which has been mentioned before.

Although the shape of the null velocity loops given by Bertin and Salmon (37) in Figure 22 and by the present investigation in Figures 23 to 26 is very similar, there is one major difference between the interpretations of the results. Bertin and Salmon (37) considered the area within the null velocity loop as the zone of recirculation. The author, on the other hand, considered the downstream end of the null velocity loop as the bisector (major axis) of the elliptical recirculation zone. The change in the velocity gradients as shown by the velocity profiles of stations 4 to 6 in Figures 23 to 26 adds further support to the interpretation of the existence of the elliptical zone of recirculation.

Also, if one considers the fluid jet as equivalent to an obstruction created by the metal baffle (as suggested by Bertin and Salmon (37)), then other conditions remaining the same, the width of the recirculation zone would be expected to be larger when the slot jet is placed with its longer side against the direction of flow instead of its short side against the direction of the mainstream flow. No such trend is observed from Figures 20 and 21, where the width of the recirculation zones with the 1/4" by 1/16" slot jet with its two different cases of orientation is presented.

Shepherd (29), in his study of flame stabilization by annular fluid jets, did one experiment to indicate the nature of the flow pattern which results in a recirculation zone. The picture of the hemispheric combustion zone given by him bears much resemblance with the visualization of the reverse zone given in the present work. Shepherd (29)

concluded: "The hemispheric portion was semitransparent before the smooth envelope broke up into a bushy yellow flame. The boundary of the recirculation zone was close to the base of this turbulent region and the plane of the reversal was quite sharp, as was indicated by traversing a salt-coated wire through the flame." In his experiments of jet stabilization by means of the outward radial flow of the stabilizing stream in an annular combustion chamber, Shepherd (29) was mainly interested in the combustion stability. Dutta, Martin and Moore (30), on the other hand, did similar jet stabilization experiments by means of inward radial flow of the stabilizing stream. They attempted to establish a relation between some characteristics of the recirculation zone and the flame stability. From experimental measurements of the axial velocity profiles across a diameter downstream of the stabilizing jet (no mention of the exact location given in their paper) in the absence of combustion, they established a characteristic dimension of the recirculation zone or the eddy region. The pilot stream was admitted at four points around the circumference of the annular chamber to ensure a uniform flow distribution for the annular jet. From the total head traverses, they estimated the penetration of the jet and hence the size of the recirculation. A typical total head traverse given by them is shown in Fig. 27. The depth of jet penetration had been taken by them to be $D-(d')/2$ where D = tube diameter and d' is the width of the uniform portion of the total head traverse curve (Figure 27). They tried to correlate their data on jet stabilization in a similar form of correlation given

previously for the bluff body flame stabilization by Spalding and Tall (39). Spalding and Tall (39) had shown that the stability data can be correlated in terms of two dimensionless groups, i.e.,

$$V_{B_o}\, d/\alpha_T = \text{constant}\, \left(\frac{Su(d)}{\alpha_T}\right)^n \qquad (17)$$

where α_T = the thermal diffusivity

n = an index depending on the Reynolds number

Su = laminar flame speed at the mixture ratio corresponding to the blowout velocity

d = baffle size.

In the jet stabilized system d had been replaced by D-d' derived from the experimental velocity traverse. The correlation between the two dimensionless numbers as plotted by Dutta, et al (30) is shown in Figure 28.

The main difference between the results of this work and the data presented for the bluff body stabilizers by Spalding and Tall (39) is that the slope is appreciably less in the present case. For bluff body stabilizers, the slope is given as 1.5 for two-dimensional stabilizers and 2.0 for three-dimensional stabilizers. The slope of the correlation curve for the bluff body system indicates (a) the dependence of stability on the size of the bluff body, and (b) the dependence of stability on the nature of the flow in the duct, i.e. on Reynolds number. In the case of jet stabilized system, the reduced slope of the correlation curve is due primarily to the presence of the stabilizing jet, which

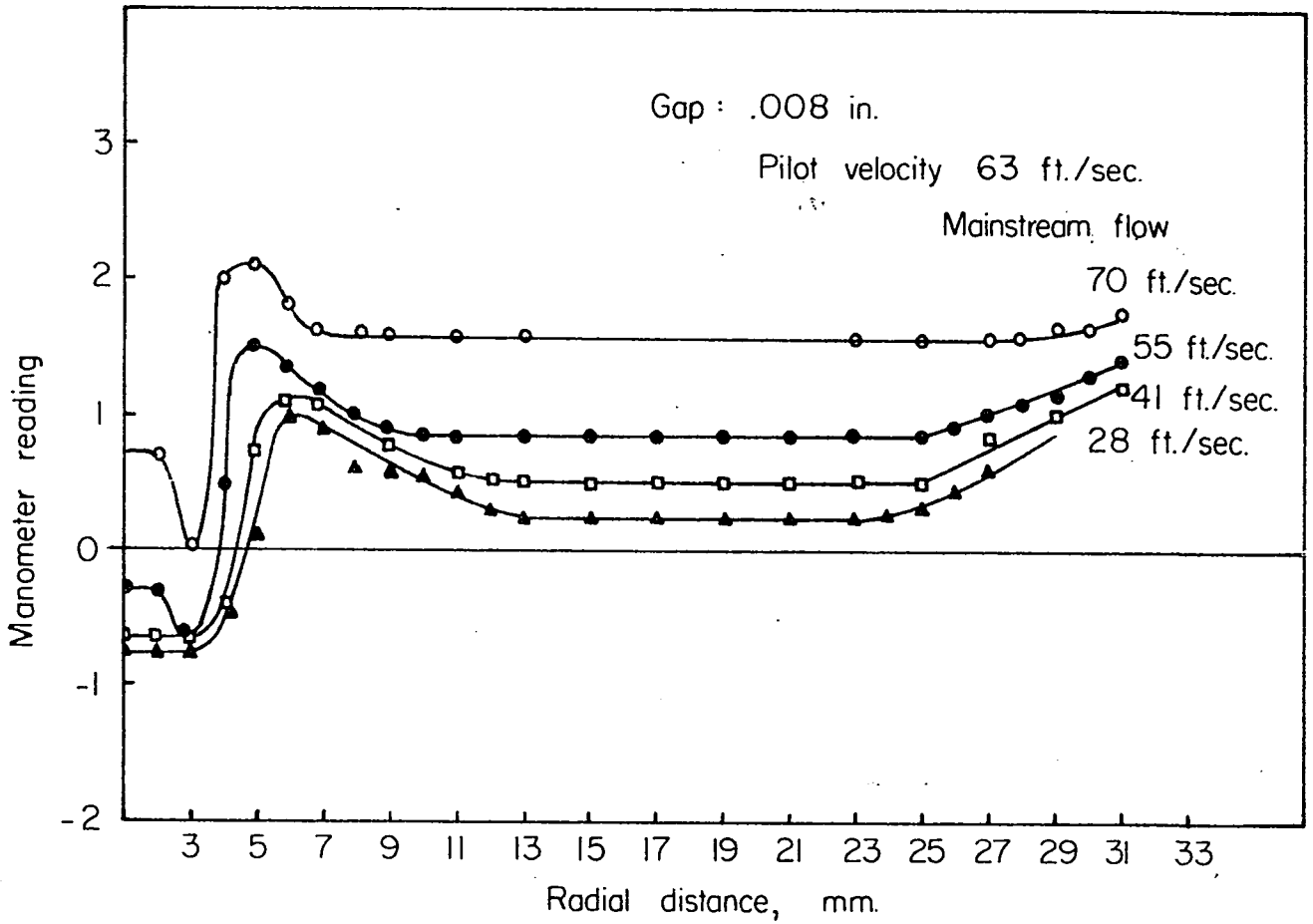

Fig. 27. Typical total head traverses in the region of recirculation (as given by Dutta, Martin and Moore)

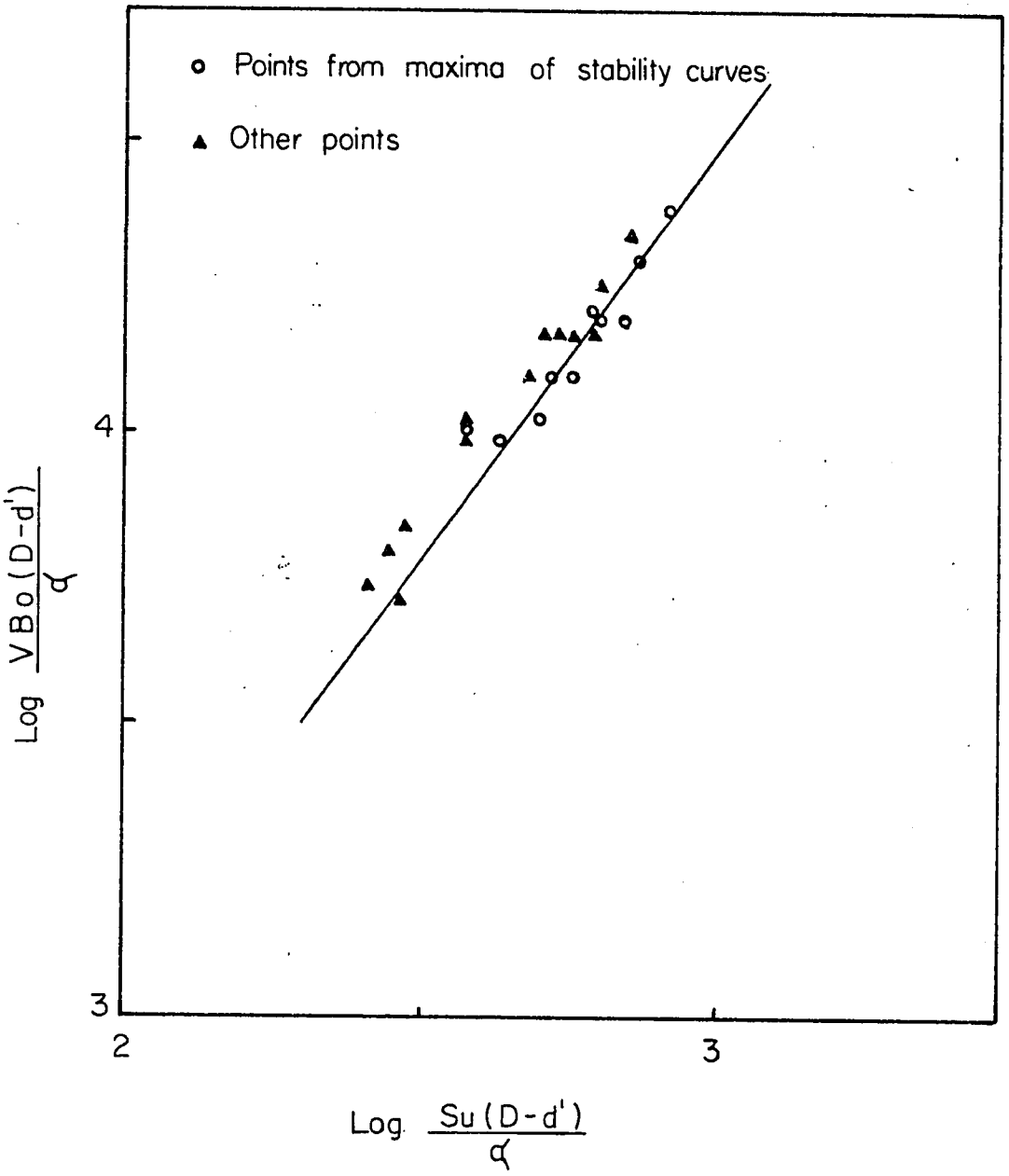

Fig. 28. Correlation of stability data
(as given by Dutta, Martin and Moore)

augments to some extent the mixing rate due merely to the presence of an obstruction in the burner tube. Dutta, et al (30) concluded that their jet stabilized system is complicated in comparison to the bluff-body system, by the presence of the stabilizing jet, whose velocity and size provide factors which, independently of the main stream flow, can influence the mixing conditions. According to them, the physical systems of the bluff body and jet stabilizations are very different.

Cambel (40) studied flame stabilization by means of opposed jet in which the tube supplying the jet gas was placed at the centre of the duct, and the jet impinged directly on the mainstream flow at an angle of 180°. The pressure of the stabilizing jet was varied from 20 psig to 180 psig, and it was seen that increased pressures increased the blowout velocity. For any particular jet tube, increasing the pressure results in a higher mass flow rate, higher efflux velocity, higher momentum and larger relative velocity between the mainstream and the stabilizing jet. Thus higher jet pressure will increase the turbulence and accelerate the mixing of the fresh main stream mixture and the partially or completely burned gases. There will be two opposing effects due to the higher jet pressure. The improved heating due to the rapid mixing is advantageous while increasing dilution will be detrimental. Thus the stabilization is related closely to the mixing processes taking place.

Flame photographs were taken and the significant distances were measured off from the photographs. The variation of flame dimensions as a function of the main stream velocity for different jet

pressures as given by Cambel (40) is reproduced in Figure 29. It is seen from this figure that flame spreading can be controlled by the pressure of the stabilizing jet. Jet pressure also influences the flame length x. For any particular main stream an increase of the jet pressure increases the flame length x, while reducing the distance b. If Cambel's jet injection system is compared with the injection system of the present investigation, then the distance x can be related with the penetration length in this investigation. And it has been seen in the experimental data that for a particular main stream velocity the penetration length increases with jet pressure.

All the penetration length data could not be taken in the present experiment because the jet often penetrated too far down in the mainstream fluid where no pressure measuring station existed. The experimental duct was designed primarily for the study of the wake flow and not for the study of the penetration lengths. However, several penetration lengths were obtained when either the jet pressures were small or the mainstream velocities were high. Table III gives the results of the penetration lengths obtained in the present work for the 1/4" by 1/8" jet. For the purpose of comparison, these penetration data are also presented in Figure 29. In this case the characteristic dimension of the slot jet (Cambel used circular jet) has been replaced by the square root of the area of the slot jet. These penetration data show the same trend as those of Cambel (40). In the author's experimental results the penetration lengths tend to converge at a high mainstream velocity. This will

happen when the mainstream rapidly bends the jet. Cambel (40) used much higher jet pressures than those of the present experiment.

Cambel (40) also mentions that for any particular set of main stream and jet stream conditions, the dimensions x and b are not greatly different for flow with and without combustion. The main change in the flow field is due to the presence of large thermal gradients in the presence of combustion. The stagnation point between the two streams and thus, the flame length, will be influenced by the jet momentum. Increasing the flame length will provide more time to entrainment of the combustion products and a longer residence time, thus favoring improved stabilization.

Though Cambel's injection system is different from the system in the present work, following his observations, it seems very probable from the results of the present experiment that flame stabilization can be achieved by means of slot jet injected from the wall of the combustion duct. There are, however, certain disadvantages in Cambel's (40) injection system. The stabilizing jet and its associated ducting are exposed to the stabilized flame and are influenced appreciably by the flame. A jet injected through the combustion chamber wall will be free from any such influence of the flame on the mechanical parts of the injection system.

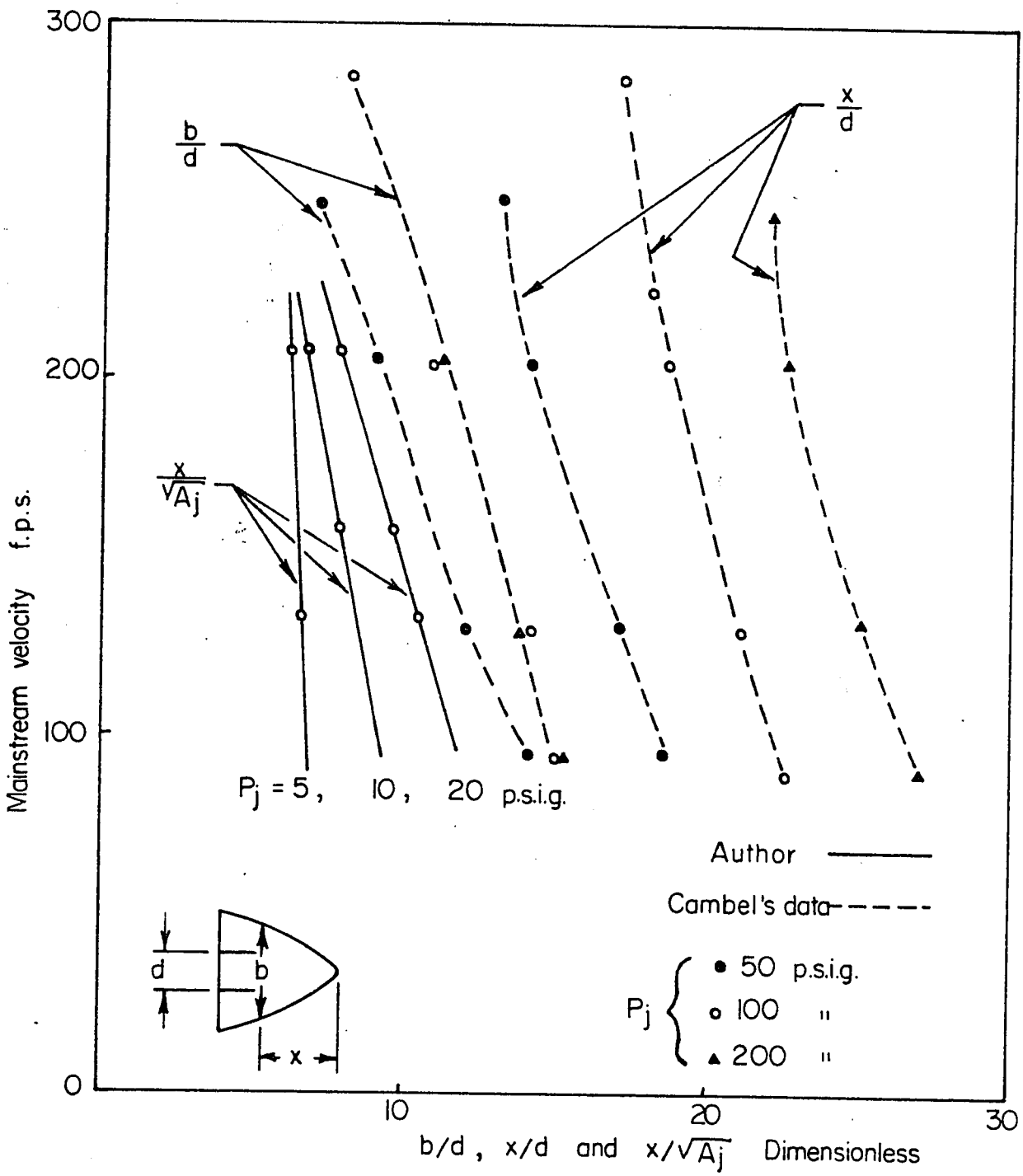
300
200
100
0
Mainstream velocity f.p.s.
b/d
x/d
x/√Aj
Pj = 5, 10, 20 p.s.i.g.
Author
Cambel's data
Pj
50 p.s.i.g.
100 "
200 "
d
b
x
10
20
30
b/d, x/d and x/√Aj Dimensionless

Fig. 29

TABLE III

Penetration lengths for the 1/4" by 1/8" jet

Jet pressure psig	Mainstream velocity F.P.S.	Penetration length at the point of injection, in.
5	132.5	1.16
15	132.5	1.75
20	132.5	1.83
5	208	1.08
10	208	1.16
20	208	1.33
30	208	1.83
5	158	1.16
10	158	1.33
20	158	1.66

The creation of a recirculation zone is only one of the many aspects of flame stabilization in a high velocity stream. Cambel (40) pointed out that the essential feature of flame stabilization by an opposed jet is the existence of a stagnant zone where the main stream of the combustible material is halted, heated and ignited. If this be the case, then one can cite that the opposed jet and bluff body flame stabilizations are basically different.

Along with the fluid dynamical condition of having a recirculation zone, proper physio-chemical conditions are equally important for successful flame stabilisation. Thus the importance of the existence of a stagnant zone of combustible material in the main stream has been well illustrated by Gammon (41). He mentioned the results of an experiment in which a streamlined two-dimensional flameholder equipped with slot jets was tested. Reverse flow along the flameholder wall occurred by the ejection of air through the slots. This recirculation zone was tried as a flameholder. However, when tested, this configuration was completely ineffective as a flameholder. In this case, the air was stagnated and not the combustible mixture. This illustrates that another necessary thing is to have the combustible material in the stagnant zone. Thus the mere presence of a recirculation zone is not sufficient for flame stabilization.

The conditions for successful flame stabilization may be given as follows:

a) fluid mass from the combustible stream should be in contact for sufficient time with the stagnated or recirculated burned or burning gases.

b) the temperature of these burned or burning gases must be high enough for rapid ignition of the combustible material within the time of contact available.

c) the velocity gradient from the source of ignition out into the main stream must be low enough for the spread of the flame into the stream.

The experimental techniques adopted by other workers to obtain the flow pattern are:

a) photographing the smoke injected with the jet, or dye injected either with the jet or with the main stream.

b) total pressure rakes to measure the velocity, or thermocouple rakes to measure the temperature when either the jet or the main stream is hot and the other is cold.

Smoke photography was employed by Chilton and Generaux (1), and by Callaghan and Ruggeri (4). This technique is quite useful for measuring the penetration of the jet. The main disadvantage here is that it gives only the picture of the outermost surface (of the wake flow) facing the duct wall and does not reveal much about what goes on at the centre of the duct width. The method of dye injection suffers from the same disadvantage. Gordier (7), in his experiments with dye injection, took pictures both from the side wall and top wall of the transparent duct. But by this means, the only additional thing he could get was the spread of the jet across the duct width.

Velocity profiles were obtained by using total pressure probe rakes and thermocouple rakes by Bertin and Salmon (37), Beauregard (9), and Chakko (8). The determination of the boundary between one hot and another cold streams by means of temperature measurement is a very sensitive measurement and hence is subject to much experimental error. Added to this will be the fact that the very existence of the thermocouple rakes is liable to change the flow pattern.

CONCLUSIONS AND COMMENTS

1. In the wake of the jet fluid a zone of recirculation is present. The fluid velocity in this zone is very much smaller than that in the mainstream flow. This is a favorable condition for a flame to exist in this zone.

2. This recirculation zone has got considerable length and breadth, which depend, primarily, on the mass velocity of the injector fluid. Thus the flame in the recirculation zone could easily ignite and spread through the surrounding fluid mass.

3. The velocity gradient in the direction of flow in the downstream of the recirculation zone is very small, and the point velocity as far down as 3" from the point of injection (farthest point to take the point velocity in the experimental setup) is less than the main stream velocity. This again is a favorable factor for the propagation of the flame through the downstream mass of the fluid.

4. By knowing the pressures, the densities, the velocities of both the main and jet streams, and the dimensions of the jet, the area and the position of the stagnant zone in the plane ABCD at the centre of the duct could be obtained from the correlations given.

5. The flow pattern in the wake of the fluid jet is vastly different from that in the wake of the conventional bluff body flame stabilizers.

6. One similarity that can be said to exist between the bluff-body and fluid jet stabilized systems is the existence of the

recirculation zone in the wake, in each case.

7. The physical and chemical characteristics of the jet stabilized system can be totally changed by changing the characteristics of the jet fluid.

8. The mechanism of recirculation is determined by both the mainstream properties and the jet properties; hence many combinations of variables can be used.

a) In actual flame stabilization it should be possible to improve the characteristics of the flame and its various zones, both physically and chemically.

b) In process industries where a rapid mixing of the reactants is desirable, jet injection may prove useful.

c) In aircraft turbojet or ramjet engines, this device of jet injection may be used as a removable flameholder. Thus a small amount of air would be bled from the engine compressor whenever the afterburner is to be used. This bleeding can be stopped whenever required, and thus there will not be any inherent drag as in the case of a bluff-body flameholder.

d) This device of stabilization by means of gaseous jets can be used as a flameholder having variable characteristics, and this flameholder could be made to operate according to the demands of different conditions during the flight of aircraft.

9. The visual study, i.e. smoke photography, dye injection, etc., of the jet mixing is not very satisfactory. In isothermal processes

the visualization of the flow regimes is not very easy in the absence of any drastic velocity gradients.

10. With the help of more complicated instruments, one should try to find the flow directions exactly in the downstream of the injector. This would help to map out the exact zone of recirculation with more accuracy. One could also extend the range of the jet dimensions investigated, and try to check this type of correlation.

NOMENCLATURE

A	=	frequency factor in the Arrhenius rate equation
A_z	=	area of the elliptical stagnant zone in square inches
A_j	=	area of the jet in square inches
C	=	a constant (approximately 10^6)
D	=	diameter of the injector, duct or the bluff body stabilizer, in inches
E	=	activation energy, in R. cals.
H_c	=	penetration length of the hot jet, in inches
K	=	apparent thermal conductivity in B.T.U. per sec. °F.
K_p	=	constant
L	=	recirculation length, in inches
P	=	pressure in pounds per sq. in.
R	=	gas constant, in ft. per °R.
R_m	=	mass velocity ratio of the side stream to the main stream
R_v	=	volume flow ratio of the side stream to the main stream
S	=	the mixing distance, in inches
S_u	=	laminar flame speed at the mixture ratio corresponding to the blowout velocity
T	=	temperature, in appropriate units
τ	=	ignition delay time, in seconds
V	=	velocity, in feet per second
V_{Bo}	=	blowoff velocity, in feet per second
X	=	distance along burner axis downstream from igniter, in inches

z = one half of the maximum jet width at a distance S downstream, in inches

b_j = width of the jet in inches

h = $\frac{\text{theoretical pilot heat}}{\text{theoretical fuel heat}} \times 100$

ℓ = penetration length, in inches

q = rate of heat input, in B.T.U. per second

x = horizontal distance from the point of injection to the point where the vertical line from the lowest point of the major axis touches the top wall, in inches.

y = vertical distance of the lowest point of the major axis of the stagnant elliptical zone from the top wall, in inches

ρ = fluid density, in pounds per cu. ft.

η_c = combustion efficiency, per cent (it compares the amount of fuel theoretically required for a given heat release to the amount actually required)

α = angle of inclination of the major axis of the elliptical zone

α_T = thermal diffusivity

Subscripts

0 = the main stream fluid

j = the jet fluid

REFERENCES

1. Chilton, T.H. and Generaux, R.P., Trans. A.I.Ch.E., 25, 102 (1930).
2. Hawthorne, W.R., Rogers, G.F.C., and Zaczek, B.Y., Roy. Aircr. Est. Tech. Note. Eng. 271 (1944).
3. Chelko, L.J., NACA RM E 50 F 21 (1950).
4. Callaghan, E.E. and Ruggeri, R.S., NACA Technical Note 1615, (June 1948).
5. Callaghan, E.E. and Bowden, D.T., NACA Technical Note 1947, (Sept. 1949).
6. Miller, E., Foster, S.P., Ross, R.W. and Wohl, K., A.I.Ch.E. Journal 3, 395 (1957).
7. Gordier, R.L., Technical Paper No. 28, Series B, University of Minnesota (August 1959).
8. Chakko, P.C., "Mixing of Hot Subsonic Jets with Cold Air Streams", M.Sc. thesis, McGill University (1956).
9. Beauregard, J.P., "The Mixing of Cold Air Jets with a Hot Gas Stream", M.Sc. thesis, McGill University (1952).
10. Ehrich, F.F., Jour. Aeronaut. Sci., 20, 99 (1953).
11. Fraser, J.P., ibid 21, 59 (1954).
12. Prandtl, L., Essentials of Fluid Dynamics, p. 135, Hafner Publ. Co. 1952.
13. Camichel, M., Engineering 123, 27 (1927).
14. Scurlock, A.C., Meteor Report, Mass. Inst. Technol., No. 19 (1948).
15. Williams, C.C., Hottel, H.C., and Scurlock, A.C., Third Symposium on Combustion, Flame and Explosion Phenomena, p. 21, William and Wilkins Publ. Co., Baltimore, 1949.
16. Nicholson, H.M., and Field, J.P., ibid. p. 44.
17. Longwell, J.P., Frost, E.E., and Weiss, M.A., Ind. Eng. Chem. 45, 1629 (1953).

18. Zukoski, E.E. and Marble, F.E., "Gas Dynamics Symposium on Aerothermochemistry, 1955", p. 205, Northwestern University, Evanston, Illinois, 1956.

19. Westenberg, A.A., Berl, W.G., and Rice, J.L., ibid, p. 211.

20. Williams, G.C. and Maddocks, F.E., Fourth Symposium (International) on Combustion, p. 727, Williams and Wilkins Publ. Co., Baltimore, 1953.

21. Wilkerson, E.C. and Fenn, J.B., ibid, p. 749.

22. Dezubay, E.A., Aero. Digest, 1950.

23. Haddock, G.W., Jet Propulsion Laboratory, Report No. 3, 24, 1951, California Institute of Technology.

24. Longwell, J.P., Chenevey, J.E., Clark, W.W., and Frost, E.E., Third Symposium on Combustion, Flame and Explosion Phenomena, Williams and Wilkins Publ. Co., Baltimore, 1949.

25. Williams, G.O., Woo, P.T. and Shipman, C.W., Sixth Symposium (International) on Combustion, p. 427, Reinhold, 1955.

26. Grover, J.H., Kesler, M.G., and Scurlock, A.C., Jet Propulsion 27, 386 (1957).

27. Ruellmantel, L.W., Ziemer, R.W., and Cambel, A.B., Jet Propulsion, 27, 31 (1957).

28. Spalding, D.B., Aircraft Engineering, 25, 264 (1953).

29. Shepherd, D.G., "Flame Stabilization by Annular Fluid Jets", Sixth Symposium (International) on Combustion, p. 472, Reinhold, 1956.

30. Dutta, B.C., Martin, D.B., and Moore, N.P.W., Sixth Symposium (International) on Combustion, p. 481, Reinhold Publ. Co., 1956.

31. Clarke, J.S., Jour. Roy. Aeron. Soc., 60, 221 (1956).

32. Schaffer, A., and Cambel, A.B., Jet Propulsion, 25, No. 6, 284 (1955).

33. Ibid, 26, No. 7, Part 1, 576 (1956).

34. Pohlman, E., M.S. Thesis, Department of Mechanical Engineering, Northwestern University, September 1954.

35. Golitzine, N., Natl. Aeronaut. Establ. Canada, Lab. Report 102, May 1954.

36. Duclos, D.P., Schaffer, A., and Cambel, A.B., Ind. Eng. Chem. 49, 2063 (1957).

37. Bertin, J., and Salmon, B., Combustion and Propulsion, 3rd AGARD Colloquium, p. 555, (1958).

38. Campbell, G.A., M.Sc. Thesis, Chemical Engineering Department, University of Ottawa, 1962.

39. Spalding, D.B., and Tall, B.S., Aero. Quart., 5, 195 (1959).

40. Cambel, A.B., 3rd AGARD Colloquium, p. 541 (1958).

41. Gammon, B.E., ibid, p. 553 (1958).

APPENDIX

SAMPLE CALCULATIONS

The Injector Velocity

For finding the velocity from the readings of a sharp-edged orifice, the formula is given by

$$V_0 = c\sqrt{\frac{2g\Delta h}{1 - (D_0/D_1)^4}}$$

or

$$V_0 = c_1\sqrt{2g\Delta h}$$

when the Reynolds number is greater than 30,000.

In the present case

$$D_0/D_1 = \frac{0.5}{0.824} = 0.61$$

For finding the value of c_1, the figure on page 63 of "Principles of Chemical Engineering" by Walker, Lewis, McAdams and Gilliland is consulted; and from there the value of c_1 is found to be 0.67.

The density of air at 10 psig and at room temperature is given by the relation

$$\rho = \frac{PM}{RT} = \frac{24.7 \times 144 \times 29}{1543 \times 530} = 0.126$$

when the reading on the manometer is 2.45 inches w.g.,

$$V_0 = 0.67\sqrt{\frac{2 \times 32.2 \times 62.4 \times 2.45}{12 \times 0.126}}$$

or

$$V_0 = 54 \text{ feet per second}$$

The velocity at the jet is given by the relation

$$V_j = \frac{A_0 V_0}{A_j} = \frac{\frac{\pi D_0^2}{4}}{A_j} V_0$$

For the 1/4" by 1/8" jet, the jet velocity

$$V_j = \frac{\frac{\pi \times 0.5^2 \times 54}{4}}{1/4 \times 1/8}$$

or

$$V_j = 340 \text{ feet per second}$$

The Point Velocity

The total pressure reading in the chart = 4.7 inches w.g.

The static pressure reading in the chart = -0.5 inches w.g.

Hence Δh = total pressure reading - static pressure reading

= 4.7 - (-0.5) = 5.2 inches w.g.

The air temperature is approximately 42 degrees Centigrade, and since the static pressure reading is small, atmospheric pressure is assumed for the calculation of air density. Therefore the density of air is

$$\frac{PM}{RT} = \frac{2118 \times 29}{1543 \times 567.6} = 0.07 \text{ lbs. per cubic foot}$$

The point velocity

$$V_x = \sqrt{2g\Delta h} = \sqrt{\frac{64.4 \times 5.2 \times 62.4}{12 \times 0.07}}$$

or

$$V_x = 153 \text{ feet per second}$$

Density of the Jet Air - ρ_j

A pressure gauge was connected at a point as close as possible to the slot jet. No pressure drop was noticed due to the air flow through the jet, i.e. the jet air discharge pressure was the same as the supply line pressure. Hence for calculation of the jet density, the pressure was taken to be equal to the supply line pressure.

Thus the density of the jet air at a supply pressure of 20 psig at room temperature is found by the relation

$$\rho_j = \frac{P_j M}{RT} = \frac{34.7 \times 144 \times 29}{1543 \times 530} = 0.177$$

EXPERIMENTAL DATA

The experimental data are presented in Tables IV to XI.

Summary of the Tabular Results

Mainstream Velocity F.P.S.	Jet Pressure psig	Jet Dimensions	Representative Table
132.5	5	1/4" x 1/16"	IV
132.5	10	1/4" x 1/16"	V
132.5	20	1/4" x 1/16"	VI
182	20	1/4" x 1/16"	VII
208	20	1/4" x 1/16"	VIII
158	20	1/4" x 1/16"	IX
132.5	5	1/4" x 1/8"	X
132.5	10	1/4" x 1/8"	XI
132.5	15	1/4" x 1/8"	XII
132.5	20	1/4" x 1/8"	XIII
208	5	1/4" x 1/8"	XIV
208	10	1/4" x 1/8"	XV
208	20	1/4" x 1/8"	XVI
208	30	1/4" x 1/8"	XVII
158	5	1/4" x 1/8"	XVIII
158	10	1/4" x 1/8"	XIX
158	20	1/4" x 1/8"	XX

TABLE V

Position A in.	Position B in.		Point Velocity F.P.S.	Position A in.	Position B in.		Point Velocity F.P.S.
7/6	5/8	downstream	49.04	7/6	1/8	downstream	55.92
4/3	3/8	"	99.31	1	3/8	"	-31.02
1	1/8	"	-49.04	1	3/4	"	37.99
1	9/8	"	58.03	7/6	10/8	"	62.04
7/6	15/8	"	75.98	4/3	15/8	"	82.07
3/2	10/8	"	106.33	4/3	10/8	"	80.59
3/2	5/8	"	118.11	2/3	5/8	"	62.04
2/3	1/8	"	-65.80	2/3	5/4	"	86.35
5/6	5/4	"	75.98	5/6	3/4	"	49.04
5/6	1/4	"	-58.03	2/3	1/8	"	-65.80
1/2	1/8	"	-67.60	1/2	3/8	"	43.87
1/2	3/4	"	71.07	1/2	9/8	"	83.52
1/2	13/8	"	90.43	1/2	17/8	"	94.34
2/3	2	"	95.61	5/6	15/8	"	90.43
1	15/8	"	80.59	7/6	19/8	"	83.52
5/6	19/8	"	95.61	1/2	19/8	"	96.85
1/6	19/8	"	80.59	1/6	13/8	"	71.07
1/6	9/8	"	58.03	1/6	5/8	"	-21.93
1/6	1/4	"	-107.45	1/3	5/4	"	79.08
1/3	1/8	"	-131.60	1/3	1/2	"	21.93
1/3	7/8	"	69.36	5/3	1/4	"	133.42
7/6	1/4	upstream	82.07	7/6	3/4	upstream	124.07
4/3	1/4	"	117.09	4/3	1/2	"	123.10
1	3/4	"	106.33	1	1/4	"	-43.87
1	1/2	"	-53.73	5/6	1/4	"	-95.61
5/6	3/4	"	21.93	5/6	1	"	131.60
2/3	3/4	"	105.19	5/6	1/2	"	-124.07
1/2	1/2	"	injector crossing				

TABLE VI

Position A in.	Position B in.	Point Velocity F.P.S.	Position A in.	Position B in.	Point Velocity F.P.S.
1/6	1/4 upstream	-156.64	1/6	1/8 downstream	-142.99
1/6	3/8 downstream	-107.45	1/6	5/8 "	-74.38
1/6	7/8 "	-49.04	1/6	9/8 "	-21.93
1/6	11/8 "	31.02	1/3	10/8 "	53.73
1/3	1 "	31.02	1/3	7/8 "	-21.93
1/3	1/8 "	-136.97	1/3	1/4 upstream	-159.68
1/3	1/2 upstream	injector crossing	1/2	3/4 "	injector crossing
1/2	1/2 "	-159.68	1/2	1/4 "	-155.09
1/2	1/8 downstream	-126.95	1/2	3/8 downstream	-84.95
1/3	3/4 upstream	111.84	1/2	1 upstream	122.12
5/6	1 "	79.08	5/6	3/4 "	-204.58
5/6	1/2 "	-136.95	5/6	1/4 "	-93.06
5/6	1/8 downstream	-53.73	5/6	3/8 downstream	21.93
1	3/8 "	37.99	1	2/8 "	31.02
1	1/8 "	-26.86	1	1/4 upstream	-79.08
1	1/2 upstream	-120.13	1	3/4 "	-148.76
1	1 "	65.80	7/6	3/4 "	-53.73
7/6	1 "	-109.67	7/6	1/2 "	51.44
2/3	1/4 "	-140.44	2/3	1/2 "	-161.18
2/3	3/4 "	injector crossing	7/6	1/4 "	-62.04
2/3	3/8 downstream	-69.36	2/3	1/8 downstream	-107.45
7/6	1/8 "	-41.03	7/6	3/8 "	21.93
8/6	1/4 "	49.04	2/3	3/4 "	31.02
2/3	5/8 "	-31.02	1/2	3/4 "	
8/6	1/4 upstream	75.98	9/6	5/8 "	69.36
9/6	10/8 downstream	69.36	9/6	14/8 "	72.74
9/6	17/8 "	77.55	10/6	17/8 "	90.43
10/6	14/8 "	93.06	10/6	10/8 "	96.85
11/6	10/8 "	117.09	11/6	5/8 "	124.07
11/6	1/8 "	126.00	9/6	1/8 "	95.61
9/6	1/4 upstream	107.45	9/6	1/2 upstream	105.19
9/6	3/4 "	118.18	9/6	1 "	132.5
7/6	1 "	116.06	7/6	3/4 "	-53.73
6/6	3/4 "	87.73	8/6	5/8 downstream	37.99
8/6	7/8 downstream	41.03	8/6	10/8 "	53.73
8/6	12/8 "	62.04	8/6	14/8 "	65.80

TABLE VI (continued)

Position A in.	Position B in.		Point Velocity F.P.S.	Position A in.	Position B in.		Point Velocity F.P.S.
1	14/8	downstream	74.38	1	12/8	downstream	69.36
1	10/8	"	62.04	1	7/8	"	46.53
7/6	3/4	"	26.86	7/6	9/8	"	49.04
7/6	11/8	"	60.07	7/6	14/8	"	69.36
5/6	11/8	"	65.80	5/6	14/8	"	75.98
7/6	17/8	"	79.08	5/6	17/8	"	83.52
5/6	1	"	51.44	2/3	14/8	"	77.55
2/3	9/8	"	53.73	2/3	11/8	"	67.60
1/2	1	"	37.99	1/2	11/8	"	67.60
1/2	13/8	"	74.38	1/3	2	"	77.55
1/3	14/8	"	72.74	1/3	12/8	"	67.60
1/6	2	"	60.07	1/6	14/8	"	51.44
1/6	12/8	"	43.87	1/6	19/8	"	67.60
1/2	19/8	"	89.09	5/6	19/8	"	87.73
7/6	19/8	"	80.59	9/6	19/8	"	80.59
11/6	19/8	"	110.76				

TABLE VII

Position A in.	Position B in.	Point Velocity F.P.S.	Position A in.	Position B in.	Point Velocity F.P.S.
5/6	1/4 downstream	49.04	5/6	1/8 downstream	-34.68
1	3/8 "	62.04	1	1/4 "	43.87
1	1/4 upstream	62.04	1	1/8 "	26.86
1/2	1/4 downstream	-138.72	1/6	1/2 "	-104.04
2/3	3/8 "	-43.87	2/3	1/2 "	37.99
1/3	5/8 "	-72.74	1/3	3/4 "	-41.03
1/3	7/8 "	46.53	1/2	5/8 "	-41.03
1/2	3/4 "	43.87	1/6	1 "	
1/3	1 "	67.60	1/2	1 "	87.73
1/2	7/8 "	71.07	2/3	7/8 "	90.43
2/3	1 "	99.31	2/3	3/4 "	82.07
2/3	5/8 "	67.60	5/6	3/8 "	74.38
5/6	5/8 "	91.75	1	1/2 "	74.38
1	3/4 "	86.35	1-1/6	3/4 "	91.75
1-1/6	3/8 "	63.95	1-1/6	1/8 "	37.99
1-1/3	1/8 "	127.89	1-1/2	1/8 "	167.04
1-1/6	1/4 upstream	150.37	1-2/3	1/8 "	183.51
1-5/6	1/8 downstream	183.51	1-5/6	3/8 "	182.85
1-2/3	3/8 "	182.72	1-1/2	1/2 "	178.86
1-1/3	1/2 "	165.59	1-1/3	3/4 "	150.37
1-1/6	1 "	105.19	1-1/2	3/4 "	178.19
5/6	1 "	107.45	1/3	1-1/8 "	106.33
1/2	1-3/8 "	100.51	1/6	1-1/4 "	106.33
1/6	1-1/2 "	84.95	1/6	1-1/4 "	65.80
1/6	1-1/8 "	49.04	1/6	7/8 "	- 43.87
1/6	5/8 "	-89.09	1/6	3/8 "	-136.09
1/6	1/8 "	-174.78	1/6	1/4 upstream	-185.46
1/6	1/2 upstream	136.09	1/3	1/2 "	injector crossing
1/2	1/2 "	injector crossing	2/3	1/2 "	injector crossing
5/6	1/2 "	-126.00	1	1/2 "	95.61
1-1/6	1/2 "	153.51	1-1/3	1/2 "	178.19
1-1/2	1/2 "	182.72	1-1/2	3/4 "	183.50
1-1/3	3/4 "	182.19	1-1/6	3/4 "	176.83
1	3/4 "	157.40	5/6	3/4 "	- 37.99
5/6	1 "	178.19	1	1 "	180.87
1-1/6	1 "	182.19	2/3	1 "	174.09
1/2	1 "	169.89	1/3	1 "	163.40
1/6	1 "	148.76	1/3	3/4 "	159.68
1/2	3/4 "	159.68	2/3	3/4 "	- 77.55
5/6	1/4 "	-112.91	1-1/3	1/4 "	172.70

TABLE VIII

Position A in.	Position B in.		Point Velocity F.P.S.	Position A in.	Position B in.		Point Velocity F.P.S.
1	1/8	downstream	147.13	5/6	1/4	downstream	-53.73
5/6	3/4	"	49.04	2/3	5/8	"	55.92
2/3	1/4	"	-102.88	1/2	1/8	"	-201.62
1/2	5/8	"	-26.86	1/3	3/8	"	-167.04
1/6	1/4	"	-196.18	1/3	3/4	"	-77.55
1/6	3/4	"	-107.45	1/6	5/4	"	26.86
1/6	15/8	"	89.09	1/6	3/2	"	65.80
1/3	17/8	"	126.95	1/3	9/8	"	72.74
1/3	13/8	"	112.91	1/6	23/8	"	111.84
1/2	19/8	"	142.04	1/2	1	"	98.09
1/2	3/2	"	123.10	2/3	17/8	"	136.97
2/3	11/8	"	117.09	5/6	3/2	"	99.31
5/6	19/8	"	124.07	1	15/8	"	113.97
7/6	5/4	"	153.53	7/6	1/8	"	190.58
5/6	23/8	"	136.09	4/3	1/8	"	206.92
3/2	1/2	"	208.08	4/3	1/2	"	204.58
3/2	7/8	"	208.08	3/2	15/8	"	204.58
5/3	7/8	"	208.08	5/3	3/4	upstream	208.08
7/6	1/2	upstream	201.02	5/6	1/2	"	87.73
1/2	1/2	"	injector crossing	1/2	3/4	"	176.15
1/6	1/2	"	147.13				

TABLE IX

Position A in.	Position B in.		Point Velocity F.P.S.	Position A in.	Position B in.		Point Velocity F.P.S.
5/3	7/8	downstream	160.43	3/2	7/8	downstream	147.13
3/2	1/8	"	154.31	5/3	1/8	"	158.16
1	1/8	"	-79.08	4/3	1/8	"	137.85
7/6	1/8	"	60.07	7/6	5/8	"	37.99
7/6	5/4	"	58.03	1	7/8	"	34.68
5/6	5/8	"	41.03	2/3	3/4	"	62.04
1/2	5/8	"	-37.99	1/2	1	"	72.74
1/3	3/4	"	-41.03	1/3	9/8	"	62.04
1/6	1	"	-34.68	1/6	11/8	"	49.04
1/6	7/4	"	69.36	1/6	19/8	"	86.35
1/6	3/8	"	-126.95	1/3	1/8	"	-172.01
1/3	3/2	"	86.35	1/3	17/8	"	104.04
1/2	19/8	"	112.91	1/2	23/8	"	118.11
1/2	7/4	"	104.04	1/2	11/8	"	94.34
2/3	1/4	"	-80.59	2/3	1	"	83.52
2/3	13/8	"	102.88	2/3	17/8	"	111.84
5/6	19/8	"	108.56	5/6	1	"	65.80
5/6	3/2	"	91.75	5/6	1/8	"	-84.95
11/6	3/8	"	162.66	11/6	3/2	"	161.18
3/2	15/8	"	129.76	4/3	13/8	"	102.88
4/3	3/4	"	112.91	4/3	17/8	"	102.88
7/6	19/8	"	93.06	7/6	27/8	"	111.84
7/6	7/4	"	79.08	1	11/8	"	67.60
1	15/8	"	86.35	1/6	1/2	upstream	118.11
1/3	1/2	upstream	injector crossing	1/3	3/4	"	136.09
1/2	3/4	"	136.97	1/2	1/4	"	-187.40
1	1/4	"	-77.55	1	1/2	"	37.99

TABLE X

Position A in.	Position B in.		Point Velocity F.P.S.	Position A in.	Position B in.		Point Velocity F.P.S.
7/6	1/4	upstream	131.60	5/6	1/4	upstream	87.73
2/3	1/4	"	-93.06	1/2	1/2	"	-111.82
1/2	3/4	"	127.89	1/3	1/2	"	100.51
5/6	3/4	"	131.60	1	1/4	"	129.76
2/3	1/4	downstream	100.51	2/3	5/8	downstream	-65.80
5/6	5/8	"	69.36	2/3	1	"	0
5/6	1	"	77.55	2/3	10/8	"	41.03
2/3	12/8	"	53.73	2/3	15/8	"	67.60
2/3	17/8	"	72.74	5/6	19/8	"	87.73
1/2	19/8	"	77.55	5/6	13/8	"	79.08
1/2	23/8	"	84.95	1/2	15/8	"	65.80
1/2	10/8	"	31.02	1/2	7/8	"	-53.73
1/2	5/8	"	-79.08	1/2	1/4	"	-122.12
1/3	1/8	"	-131.60	1/3	5/8	"	-82.07
1/6	1/8	"	-133.42	1/6	5/8	"	-82.07
1/6	10/8	"	-21.93	1/3	10/8	"	34.68
1/3	15/8	"	69.36	1/6	13/8	"	43.87
1/6	2	"	58.03	1/5	25/8	"	75.98
1/3	17/8	"	74.38	1/6	18/8	"	63.95
5/6	23/8	"	90.43	1	17/8	"	105.19
1	10/8	"	109.67	7/6	10/8	"	129.76
8/6	5/8	"	131.60	1	1/4	"	120.13
7/6	1/8	"	131.60	7/6	5/8	"	129.76
8/6	1	"	130.68	9/6	1	"	131.60
5/6	1/8	"	79.08	1/6	1/2	upstream	111.84

TABLE XI

Position A in.	Position B in.		Point Velocity F.P.S.	Position A in.	Position B in.		Point Velocity F.P.S.
5/6	1/8	downstream	113.97	1	1/8	downstream	41.03
7/6	1/8	"	108.56	8/6	1/8	"	129.76
9/6	1/8	"	131.60	9/6	5/8	"	131.60
9/6	3/8	"	131.60	8/6	5/8	"	123.10
9/6	10/8	"	130.68	7/6	10/8	"	87.73
1	9/8	"	51.44	1	1/2	"	43.87
5/6	5/8	"	-60.07	5/6	3/8	"	-82.07
5/6	1	"	-21.93	5/6	10/8	"	31.02
5/6	13/8	"	51.44	5/6	17/8	"	65.80
1	15/8	"	69.36	5/6	23/8	"	79.08
5/6	19/8	"	71.07	2/3	3/8	"	-98.09
1/6	1/4	"	-129.76	1/3	1/8	"	-140.44
1/3	1/2	"	-102.88	1/2	3/8	"	-107.45
1/2	3/4	"	-62.04	1/2	9/8	"	26.86
2/3	10/8	"	34.68	2/3	12/8	"	51.44
1/2	13/8	"	63.95	2/3	3/4	"	-62.04
1/3	3/4	"	-74.38	1/6	7/8	"	-65.80
1/6	10/8	"	-26.86	1/3	9/8	"	-21.93
1/3	15/8	"	65.80	1/2	2	"	74.38
2/3	15/8	"	63.95	2/3	17/8	"	71.07
1/6	2	"	49.04	1/6	12/8	"	21.93
1/6	19/8	"	60.07	1/3	12/8	"	49.04
7/6	14/8	"	83.52	7/6	19/8	"	87.73
5/6	1/2	upstream	-129.76	5/6	3/4	upstream	118.11
1	1/2	"	62.04	7/6	1/4	"	107.45
1/3	1/2	"	-153.53				

TABLE XII

Position A in.	Position B in.		Point Velocity F.P.S.	Position A in.	Position B in.		Point Velocity F.P.S.
7/6	19/8	downstream	65.80	5/6	19/8	downstream	75.98
1/2	19/8	"	32.07	1/6	19/8	"	51.44
1/3	17/8	"	63.95	1/2	15/8	"	67.60
2/3	13/8	"	60.07	5/6	11/8	"	34.68
1	5/4	"	-21.93	7/6	1	"	-26.86
4/3	3/4	"	71.07	3/2	5/8	"	118.11
3/2	1/8	"	124.07	5/3	1/8	"	129.76
11/6	3/8	"	132.51	11/6	1/8	"	131.60
5/3	1	"	128.83	11/6	7/8	"	132.51
11/6	15/8	"	128.83	5/2	15/8	"	133.42
5/3	17/8	"	117.09	3/2	15/8	"	96.85
4/3	5/4	"	71.07	4/3	17/8	"	74.38
3/2	25/8	"	99.31	7/6	15/8	"	58.03
7/6	23/8	"	77.55	7/6	3/2	"	43.87
1	17/8	"	63.95	1	7/4	"	51.44
5/6	15/8	"	65.80	2/3	2	"	75.98
2/3	9/8	"	0	2/3	5/8	"	-90.43
2/3	1/8	"	-143.83	1/2	5/4	"	31.02
1/2	7/8	"	-65.80	1/2	5/8	"	-94.34
1/3	3/4	"	-87.73	1/3	3/8	"	-129.76
1/3	5/4	"	-21.93	1/3	13/8	"	-46.53
1/6	7/4	"	26.86	1/6	5/4	"	-50.02
1/6	5/8	"	-98.09	1/6	1/8	"	-153.53
1/2	1/4	upstream	-148.76	2/3	1/2	upstream	injector crossing
5/6	1/2	"	-138.72	1	3/4	"	43.73
7/6	1/2	"	34.68	4/3	1/2	"	108.56
4/3	1/8	downstream	105.19	7/6	1/4	downstream	-69.36

TABLE XIII

Position A in.	Position B in.		Point Velocity F.P.S.	Position A in.	Position B in.		Point Velocity F.P.S.
4/3	5/8	downstream	-63.95	3/2	1/8	downstream	80.59
4/3	1/8	"	-89.09	7/6	1/8	"	-127.89
3/2	1/2	"	58.03	1	1/4	"	-128.83
5/6	1/8	"	-150.37	2/3	1/4	"	-144.66
1/2	1/8	"	-161.18	1/3	1/4	"	-158.16
1/6	1/8	"	-165.59	1/6	5/8	"	-106.33
1/6	5/4	"	-55.92	1/3	3/4	"	-96.09
1/2	7/8	"	-82.07	2/3	7/8	"	-79.08
5/6	7/8	"	-72.74	1	1	"	-63.95
7/6	3/4	"	-77.55	7/6	5/4	"	-41.03
4/3	5/4	"	26.86	3/2	5/4	"	53.73
5/3	5/4	"	95.61	11/6	5/4	"	120.13
11/6	1/8	"	134.31	5/3	3/8	"	117.09
5/3	1/8	"	125.04	11/6	3/8	"	132.51
12/6	17/8	"	105.19	5/3	15/8	"	83.52
2	17/8	"	128.83	3/2	7/4	"	55.92
4/3	13/8	"	26.86	4/3	17/8	"	51.44
7/6	15/8	"	46.53	4/3	15/8	"	41.03
3/2	17/8	"	62.04	7/6	17/8	"	58.03
7/6	19/8	"	63.95	5/6	19/8	"	80.59
1	17/8	"	63.95	1	13/8	"	34.68
5/6	15/8	"	65.80	5/6	3/2	"	41.03
5/6	9/8	"	-46.53	2/3	9/8	"	-49.04
2/3	3/2	"	41.03	2/3	15/8	"	67.60
2/3	17/8	"	77.55	1/2	19/8	"	79.08
1/2	5/4	"	-31.02	1/2	13/8	"	49.04
1/2	2	"	65.80	1/3	9/8	"	-60.07
1/3	3/2	"	21.93	1/3	15/8	"	51.44
1/3	17/8	"	62.04	1/6	19/8	"	51.44
1/6	15/8	"	26.86	1/3	1/4	upstream	-171.30
1/2	1/2	upstream	injector crossing	5/6	1/2	"	-171.30
1	1/4	"	-155.09	3/2	3/4	"	102.88
1/3	3/4	"	121.13	2/3	3/4	"	injector crossing
2/3	1	"	126.95	1	3/4	"	injector crossing
1	1	"	129.76	4/3	3/4	"	71.07
4/3	1/4	"	21.93				

TABLE XIV

Position A in.	Position B in.	Point Velocity F.P.S.	Position A in.	Position B in.	Point Velocity F.P.S.
2/3	1/8 downstream	178.19	1/2	1/4 downstream	-87.73
2/3	3/8 "	173.40	1/2	3/4 "	-75.98
1/2	5/4 "	75.98	1/3	9/8 "	-37.99
1/3	13/8 "	93.06	1/3	17/8 "	116.06
1/2	15/8 "	115.02	1/2	19/8 "	131.60
5/6	19/8 "	190.58	5/6	5/8 "	198.61
5/6	5/4 "	198.61	1	1/8 "	204.58
7/6	1/8 "	208.08	7/6	5/8 "	208.08
1/3	1/8 "	-208.08	1/3	5/8 "	-136.09
1/6	1/2 "	-149.57	1/6	5/4 "	49.04
1/6	15/8 "	101.70	1/6	7/8 "	-75.98
1/2	1/2 upstream	188.68	1/3	1/4 upstream	injector crossing
1/2	1/4 "	21.93	1/3	1/2 "	176.83
1/6	1/4 "	injector crossing	1/6	1/2 "	150.37

TABLE XV

Position A in.	Position B in.		Point Velocity F.P.S.	Position A in.	Position B in.		Point Velocity F.P.S.
5/6	1/8	downstream	198.01	1	1/8	downstream	199.22
7/6	1/8	"	208.08	7/6	3/8	"	208.08
1	3/8	"	204.58	1	5/4	"	198.01
7/6	9/8	"	208.08	5/6	9/8	"	165.59
2/3	7/8	"	69.36	1/2	5/8	"	-123.10
1/3	3/4	"	-110.76	1/3	5/4	"	49.04
1/2	5/4	"	37.99	2/3	5/4	"	94.34
2/3	15/8	"	118.11	1/2	3/2	"	72.74
1/2	7/8	"	-84.95	1/3	7/8	"	-86.35
1/3	3/2	"	82.07	1/6	13/8	"	74.38
1/6	5/4	"	-21.93	1/6	5/8	"	-131.60
1/3	17/8	"	116.06	1/2	2	"	104.04
1/6	19/8	"	104.04	1/2	1/8	"	-210.38
2/3	3/8	"	62.04	1/6	1/2	upstream	147.95
1/3	1/2	upstream	169.89	1/2	1/2	"	169.89
2/3	1/2	"	196.71	2/3	1/4	"	184.16
1/3	1/4	"	injector crossing	1	1/2	"	205.75
4/3	1/2	"	209.80				

TABLE XVI

Position A in.	Position B in.		Point Velocity F.P.S.	Position A in.	Position B in.		Point Velocity F.P.S.
5/6	1/8	downstream	-202.22	7/6	1/8	downstream	199.82
4/3	1/8	"	207.50	5/6	7/8	"	-72.74
1	3/4	"	37.99	1	1/4	"	53.73
1	5/4	"	75.98	1	2	"	108.56
5/6	17/8	"	98.09	5/6	3/2	"	43.87
2/3	5/4	"	-31.02	2/3	13/8	"	77.55
2/3	17/8	"	113.97	1/2	3/2	"	72.74
1/2	2	"	113.97	1/2	1	"	-93.06
1/2	19/8	"	128.83	1/3	17/8	"	101.70
1/3	13/8	"	60.07	1/3	9/8	"	-90.43
1/6	5/4	"	-90.43	1/6	7/4	"	0
1/6	19/8	"	80.59	1/6	3/4	"	-144.66
1/6	1/4	"	-214.90	4/3	5/8	"	208.08
4/3	2	"	186.11	5/3	15/8	"	210.95
5/3	3/8	"	210.38	4/3	5/4	"	199.22
2/3	5/8	"	-155.87	1/2	3/8	"	-200.42
1/3	5/8	"	-158.16	3/2	7/8	"	208.65
4/3	1/2	upstream	208.08	1	1/2	upstream	172.70
1/6	1/2	"	161.16	1/2	1/2	"	injector crossing
1/2	3/4	"	186.76	2/3	1/2	"	injector crossing
5/6	3/4	"	199.22	1	1/4	"	178.19

TABLE XVII

Position A in.	Position B in.		Point Velocity F.P.S.	Position A in.	Position B in.		Point Velocity F.P.S.
3/2	7/8	downstream	147.13	5/3	1/8	downstream	203.40
11/6	1/8	"	204.58	7/6	1/8	"	-151.16
3/2	1/8	"	186.11	4/3	1/8	"	96.85
4/3	5/4	"	69.36	7/6	5/4	"	-43.87
7/6	15/8	"	69.36	4/3	15/8	"	87.73
3/2	15/8	"	118.11	5/3	17/8	"	155.09
3/2	19/8	"	124.07	11/6	19/8	"	184.81
7/6	19/8	"	96.85	5/6	19/8	"	117.09
1/2	19/8	"	117.09	1/6	19/8	"	72.74
1/6	15/8	"	43.87	1/3	7/4	"	72.74
1/2	15/8	"	94.34	2/3	7/4	"	86.35
5/6	13/8	"	71.07	1	15/8	"	72.74
1	5/4	"	-69.36	5/6	9/8	"	-82.07
2/3	5/4	"	-31.02	1/2	11/8	"	0
1/3	5/4	"	-69.36	1/6	5/4	"	-91.75
1/6	5/8	"	-161.18	1/6	1/8	"	injector crossing
1/3	3/8	"	-206.38	1/2	5/8	"	-160.43
2/3	3/4	"	-136.97	5/6	5/8	"	-147.13
5/6	1/8	"	-220.43	1	3/8	"	-169.19
7/6	3/4	"	-99.31	1/2	1	"	-94.34
7/6	1/4	upstream	-135.21	7/6	1/2	upstream	-128.83
7/6	3/4	"	65.80	4/3	1/2	"	90.43
4/3	3/8	"	174.09	1/6	1/2	"	150.37
1/3	3/4	"	178.19	2/3	3/4	"	156.64
5/6	1/2	"	injector crossing	1	3/4	"	-126.95

TABLE XVIII

Position A in.	Position B in.		Point Velocity F.P.S.	Position A in.	Position B in.		Point Velocity F.P.S.
1/2	1/8	downstream	-158.92	2/3	1/8	downstream	127.89
5/6	1/8	"	151.16	1	1/8	"	155.09
7/6	1/8	"	156.64	7/6	5/8	"	158.16
7/6	5/4	"	156.64	7/6	19/8	"	157.40
1/2	19/8	"	98.09	1/2	5/8	"	-87.73
1/2	5/4	"	49.04	1/2	13/8	"	74.38
1/3	3/4	"	-80.59	1/3	9/8	"	34.68
1/3	3/2	"	71.07	1/3	17/8	"	94.34
1/6	19/8	"	86.35	1/6	13/8	"	63.95
1/6	7/8	"	-71.07	1/6	1/4	"	-151.96
1/3	1/8	"	-159.68	2/3	7/8	"	65.80
2/3	15/8	"	96.85	5/6	19/8	"	125.04
5/5	5/4	"	129.76	1	3/4	"	155.09
1	13/8	"	150.37	3/2	5/4	"	159.68
1/6	1/2	upstream	118.11	1/2	1/2	upstream	145.49
5/6	1/4	"	151.96	3/2	3/4	"	159.68

TABLE XIX

Position A in.	Position B in.		Point Velocity F.P.S.	Position A in.	Position B in.		Point Velocity F.P.S.
5/6	1/8	downstream	43.87	2/3	1/8	downstream	47.13
2/3	5/8	"	-83.52	5/6	5/8	"	46.53
5/6	5/4	"	71.07	2/3	5/4	"	37.99
1/2	7/8	"	-62.04	1/2	11/8	"	55.92
1/2	3/8	"	-126.00	1/3	1/4	"	-155.09
1/3	3/4	"	-89.09	1/3	9/8	"	0
1/3	13/8	"	74.38	1/3	17/8	"	93.06
1/6	19/8	"	80.59	1/6	7/4	"	55.92
1/6	5/4	"	-31.02	1/6	5/8	"	-107.45
1/6	1/8	"	-165.59	7/6	1/8	"	148.76
4/3	1/8	"	158.16	4/3	5/8	"	158.16
4/3	15/8	"	158.16	3/2	5/4	"	160.43
11/6	5/8	"	161.18	7/6	7/8	"	147.13
7/6	19/8	"	136.97	1	15/8	"	110.76
1	1	"	116.06	11/6	19/8	"	161.18
5/6	7/4	"	79.08	5/6	19/8	"	93.06
2/3	13/8	"	63.95	2/3	17/8	"	83.52
1/2	15/8	"	83.52	1/2	19/8	"	96.85
1/6	1/2	upstream	118.11	1/2	1/2	upstream	145.49
5/6	1/4	"	151.96	3/2	3/4	"	159.68
1	1/4	"	126.00				

TABLE XX

Position A in.	Position B in.		Point Velocity F.P.S.	Position A in.	Position B in.		Point Velocity F.P.S.
1	1/2	downstream	-124.07	3/2	1/8	downstream	148.76
11/6	1/8	"	161.18	5/3	1/8	"	158.16
5/3	5/8	"	158.16	5/6	5/8	"	-120.13
1	7/8	"	-91.75	1	3/2	"	21.93
1	15/8	"	60.07	7/6	5/4	"	-43.87
7/6	5/8	"	-94.34	7/6	7/4	"	46.53
4/3	15/8	"	69.36	7/6	19/8	"	77.55
4/3	7/8	"	43.87	3/2	5/4	"	109.67
3/2	19/8	"	96.85	5/3	17/8	"	125.04
11/6	19/8	"	147.95	1	17/8	"	77.55
5/6	19/8	"	98.09	5/6	7/4	"	72.74
5/6	9/8	"	-62.04	5/6	1/8	"	-174.09
1/6	3/8	"	-90.43	1/3	1/8	"	-120.13
2/3	1/8	"	-129.76	2/3	3/4	"	-49.04
1/2	5/8	"	-49.04	1/3	5/8	"	-67.60
1/6	7/8	"	21.93	1/6	5/4	"	-31.02
1/6	15/8	"	51.44	1/6	19/8	"	67.60
1/3	17/8	"	82.07	1/3	9/8	"	31.02
1/3	13/8	"	67.60	1/2	19/8	"	102.88
1/2	7/4	"	89.09	1/2	5/4	"	69.36
2/3	5/4	"	67.60	2/3	15/8	"	91.75
2/3	17/8	"	107.45	1	1/4	upstream	-174.09
1	3/4	upstream	-125.04	1	1	"	161.92
7/6	3/4	"	89.09	7/6	1/4	"	-116.06
4/3	1/4	"	125.04	5/6	1	"	160.43
1/2	3/4	"	130.68	1/3	1/2	"	-105.19